

Dynamic modeling and control strategies of organic Rankine cycle systems: Methods and challenges

Muhammad Imran^{1,2,*}, Roberto Pili², Muhammad Usman³, Fredrik Haglind²

¹*Mechanical Engineering & Design, School of Engineering and Applied Science, Aston University, Aston Triangle, B4 7ET Birmingham, United Kingdom*

²*Department of Mechanical Engineering, Technical University of Denmark, Nils Koppels Alle, Building 403, 2800 Kongens Lyngby, Denmark*

³*Centre of Advanced Powertrain and Fuels, Department of Mechanical, Aerospace, & Civil Engineering, Brunel University, UB8 3PH London, United Kingdom*

Abstract

Organic Rankine cycle systems are suitable technologies for utilization of low/medium-temperature heat sources, especially for small-scale systems. Waste heat from engines in the transportation sector, solar energy, and intermittent industrial waste heat are by nature transient heat sources, making it a challenging task to design and operate the organic Rankine cycle system safely and efficiently for these heat sources. Therefore, it is of crucial importance to investigate the dynamic behavior of the organic Rankine cycle system and develop suitable control strategies. This paper provides a comprehensive review of the previous studies in the area of dynamic modeling and control of the organic Rankine cycle system. The most common dynamic modeling approaches, typical issues during dynamic simulations, and different control strategies are discussed in detail. The most suitable dynamic modeling approaches of each component, solutions to common problems, and optimal control approaches are identified. Directions for future research are provided. The review indicates that the dynamics of the organic Rankine cycle system is mainly governed by the heat exchangers. Depending on the level of accuracy and computational effort, a moving boundary approach, a finite volume method or a two-volume simplification can be used for the modeling of the heat exchangers. From the control perspective, the model predictive controllers, especially improved model predictive controllers (e.g. the multiple model predictive control, switching model predictive control, and non-linear model predictive control approach), provide excellent control performance compared to conventional control strategies (e.g. proportional–integral controller, proportional–derivative controller, and proportional–integral–derivative controllers). We recommend that future research focuses on the integrated design and optimization, especially considering the design of the heat exchangers, the dynamic response of the system and its controllability.

Keywords: Organic Rankine cycle, Control, Dynamic modeling, PID, Model predictive control, Optimized control, Non-linear control, Finite volume and moving boundary, Robust control

* Corresponding Author
m.imran12@aston.ac.uk

1. Introduction

The future energy demand of the ever-increasing global population requires efficient utilization of current energy resources as well as the development of sustainable energy solutions. The conversion of energy, from primary energy sources to end use, involves several losses that result in waste heat to the environment. Waste heat resources for organic Rankine cycle (ORC) systems are normally classified into three categories [1]:

- 1) Low-grade or low-temperature waste heat (ambient – 250 °C);
- 2) Medium temperature waste heat (250 °C – 500 °C);
- 3) High temperature waste heat (> 500 °C).

It is estimated that 72 % of the primary energy consumption is discarded as waste heat, and about 78 % of the waste heat is low-grade heat or low-temperature heat [2]. For energy efficiency improvement and reduction of the overall energy consumption, the conversion of waste heat to power can play an important role. The low-grade thermal energy cannot be converted efficiently to electrical power by conventional energy conversion technologies (Steam Rankine or Brayton cycle), and a large amount of low-temperature heat sources remain untapped. These low-grade thermal energy and waste heat resources include heat from energy conversion plants based on renewable energy sources as well as waste heat from industries, thermal power plants, and the transportation sector.

The conversion of low-grade thermal energy and waste heat to power can provide financial benefits for the plant owner, as well as improve energy efficiency and reduce CO₂ emissions of the plant [3]. Among the existing technologies to convert low-grade heat to power, the organic Rankine cycle (ORC) can be considered an ideal technology. The ORC systems have the following unique features:

- Adaptability to various heat sources
- Advantages with respect to common steam Rankine cycle systems for heat source temperature below 300-400 °C and small scale (below 5 MW)
- Proven technology
- Suitability for distributed power generation
- Usable over a wide capacity range (a few kW to a few MW)
- Good part-load performance
- Low complexity
- Experienced manufacturers and technology providers
- Extensive market potential

Geothermal energy, waste heat from various thermal processes, biomass combustion, solar energy and ocean thermal energy are the major heat sources for the ORC technology [4]. A number of review studies

have been reported for the ORC technology regarding waste heat recovery (WHR) from internal-combustion engines (ICE) [5], and for maritime applications [6].

WHR from gas turbines in compressed gas stations is also an important field of application for ORC, as reported in [7] and [8]. Hoang A. T. [9] presented a comprehensive review of the component design and economic feasibility of ORC for waste heat recovery from diesel engines. Shi et al. [10] reviewed the different configurations of the ORC system based on heat source temperature and nature of the working fluids for waste heat recovery from internal-combustion engines. Lion et al. [11] provided a comprehensive review of the application of ORC technology on a heavy-duty diesel engine with particular focus on vehicle applications for on and off highway sectors. The paper also provided operating profiles (engine torque and speed) and used them to assess the emissions with and without an ORC system. Zhou et al. [12] provided a detailed review of the ORC system for passenger vehicles and outlined the major challenges for ORC integration. Zhai et al. [13] provided a theoretical categorization of heat sources based on the heat source availability, and the type, temperature, capacity, and dynamics of the heat source. Lecompte et al. [14] reviewed the typical and innovative ORC architectures for WHR. The authors identified the difficulty in assessing the additional complexity and the importance of evaluating also the economic feasibility of new architectures rather than focusing only on thermodynamic analysis.

The core research in the field of ORC technology can be broadly classified into working fluids, expansion machines, cycle configuration, design, experimental investigation, optimization, and dynamic modeling and control of the ORC system [15]; see Table 1. It can be observed that a significantly large area of work is within the domain of optimization and design. However, in the open literature, the dynamic modeling and control studies constitute less than 10% of the total number of publications in the area of ORC technology [16,17].

Table 1. Major research areas in ORC technology, Park et al. [17].

Research area	Number of publications in ORC technology (normalized number of papers published in the area divided by total papers published in the ORC field)
Design/Modeling/Analysis	0.369
Optimization	0.139
Expander/Turbine	0.148
Working fluid	0.126
Dynamics	0.031
Control	0.030
Pump	0.018
Heat exchanger	0.016
Cycle configuration	0.009

The dynamic modeling and control aspects are critically important for ORC systems that are subjected to changes in the heat source or cold sink conditions. ORC systems operated in off-grid/island-mode need to react to load changes as well. Fluctuating primary heat sources (mass flow rate or temperature) include solar thermal, waste heat recovery from industries, waste heat recovery from internal-combustion engines of heavy-duty vehicles and gas turbines in compressed gas stations. The use of transient heat sources can lead to over-heating, causing fluid decomposition of the working fluid of the ORC, and component failure of the ORC due to stalling or temperature shocks. With respect to WHR from a diesel engine, the transient heat source may result in operational difficulties of the emission-control system during start-up and shutdown procedures. In addition, frequent and rapid changes of the heat source force the ORC system to operate far from the design-point, thus deteriorating its performance and economic potential. Storage solutions might be used, but the additional capital costs for the storage might affect the economic feasibility of the WHR.

Furthermore, it is known that for isentropic or dry working fluids, a decrease in the degree of working fluid superheating at the turbine inlet leads to an increase in the thermal efficiency, if the ORC does not preheat the working fluid with an internal heat exchanger (recuperator) [18]. However, operating the ORC using a turbo-expander with a very small degree of superheating may lead to erosion on the turbine blades as the fluctuations in the heat source conditions may lead to incomplete evaporation of the working fluid. The potential occurrence of turbine erosion is governed by the system thermal inertia and configuration. Thus, the estimation of operational parameters such as superheating and its sensitivity to heat source fluctuation and load conditions require rigorous analysis of the process dynamics. The data for such dynamic studies can be obtained from experimental work, but the cost of constructing test rigs is generally high. Moreover, often sub-optimal control schemes are employed in experimental work for safety concerns. In order to resolve the aforementioned barriers, it is of crucial importance to understand the dynamic response of the system and develop suitable controllers ensuring safe operation, long life of the ORC unit and maximum performance under varying heat source and cold sink conditions.

To some extent, the expertise and guidelines concerning the dynamic modeling of ORC systems can be obtained from the fields of steam power plants, gas turbine engines, and combined cycle power plants [19,20]. However, these power plants typically operate close to the design point, whereas ORC systems utilizing fluctuating heat sources often operate far from the design point depending on the heat source, cold sink and loading conditions.

A literature review indicates that the dynamic modeling and control of ORC systems have evolved from component-level analyses in the last decade and are now mature enough to simulate complex ORC systems with the integration of components. However, despite the availability of specific studies, there is no previous work presenting a holistic picture of the state-of-the-art on the topic.

The lack of a review critically evaluating and comparing the different dynamic modeling and control approaches, makes it difficult for researchers and industry developers to make the appropriate choices with regards to these methods, hindering the development of optimal controllers for ORC systems that encounter highly transient heat sources. Consequently, the lack of a holistic review may impede the commercialization of ORC systems for applications characterized by highly transient heat sources (e.g. the truck industry).

This paper provides a comprehensive review of the dynamic modeling and control of ORC systems. The component-level modeling is discussed, as well as the integration of components to form and model complex systems; the technical difficulties, simulation pitfalls, best practices, and different modeling techniques are presented in detail. Various control schemes are compared, and the advantages, disadvantages and maturity level for each of them are discussed. The more suitable dynamic models of each component, solutions to common problems, and optimal control approaches are identified. Directions for future research are provided. Overall, the paper provides a unique, unified reference benchmark for future work concerning dynamic modeling and control of ORC systems.

The paper consists of five sections. The introduction and state-of-the-art review are presented in Section 1. Section 2 discusses the common dynamic modeling approaches of ORC systems, both at the component and the system-level. The control approaches for ORC systems and their merits and demerits are discussed in Section 3. Dynamic modeling and controller development tools and software are covered in Section 4. Finally, the concluding remarks are presented in Section 5.

2. Dynamic modeling

This section provides a detailed description of the methodology and state-of-the-art approach used for the dynamic modeling of the ORC components, namely, the heat exchangers (evaporator and condenser), expander, pump, control valves, and storage tank. The modeling of single-phase heat exchangers, such as preheaters, subcoolers and recuperators, can be derived from the evaporator and condenser models, considering that the working fluid is found only at the liquid or only at the vapor phase under normal operation.

The control of the ORC system is based on its dynamic response. Therefore, understanding the process dynamics plays a critical role for a successful controller design. The dynamic response of the ORC system depends on a number of factors, such as cycle configuration, type of the components, and working fluid.

The modeling paradigm to study the dynamics of the ORC technology used today is mostly modular, rather than simultaneous. The principle of modularity implies that the outputs of a module (component model) must be dependent on the inputs of the module and be a function of internal parameters only. This allows for the reusability of a model and for using a bottom-up approach to develop libraries of

components for easy application and reconfiguration. On the other hand, the use of a simultaneous modeling approach fixes the system as a whole and generates a computationally efficient code; however, this technique does not allow modifications to be easily done to the model, and the set of equations needs to be rewritten if a component is added.

The interest in dynamic modeling goes back to 2007 when Colonna et al. [19,20] presented a dynamic modeling paradigm for a steam Rankine cycle and experimentally validated the results against measurements from a steam power plant. Wei et al. [21] presented two alternative approaches for a dynamic model for the design of heat exchangers of an ORC unit in 2007. Quoilin et al. [22] presented a dynamic model and control strategy for a varying heat source in 2011. In 2013, Casella et al. [23] presented a software library [24] including modular, reusable ORC components which were experimentally validated against a commercial ORC unit. Later, Quoilin et al. [25] reported the development of a library for the dynamic simulation of thermodynamic systems in the object-oriented language Modelica. Pierobon et al. [26] presented a novel approach to integrate the dynamic performance of the ORC system into the preliminary design phase. The numerical model performed the thermodynamic cycle calculation and the design of the components of the system. The results of these simulations were used within the framework of a multi-objective optimization procedure to identify a number of equally optimal system configurations. A dynamic model of each of these systems was automatically parameterized, by inheriting its parameter values from the design model. Lakhani et al. [27] presented a dynamic modeling scheme of an ORC-based solar thermal power system with an integrated multi-tube shell and tube thermal storage system in 2017. Recently, Hustler et al. [28] presented a validated dynamic model of an ORC unit for waste heat recovery in a diesel truck. In addition, the thermo-physical properties of the working fluids (such as heat capacity, latent heat, critical temperature, and density) affect the dynamic response of the ORC system. Shu et al. [29] investigated the dynamic response of 14 different working fluids based on the rise time, settling time and time constant. The results suggest that the working fluids with low critical temperature provide a faster response than those of working fluids with a high critical temperature.

Colonna et al. [19] recognized a difference between simultaneous and modular paradigms classifying the causal and non-causal models. In causal models, the systems are decomposed into computational blocks with predefined causal interactions. This implies that input variables to the system must be decided prior to the development of the overall model, and the resulting model will have certain rigidity tied to the boundary and initial conditions, resulting in an explicit state-space form. However, bilateral coupling, discussed in detail in Ref. [19], can be used to choose input and output variables. The early computer solvers were able to work with causal models only, and often there was a need to manually reduce differential algebraic equations (DAEs) to ordinary differential equations (ODE), increasing chances of errors and modeling efforts. Modern solvers can handle non-causal models and simplify the

models using computer algebra and reorder the equations depending upon the choice of input and output variables, simplifying the work for the user.

The ORC component modeling generally involves the solution of three conservation equations for each component, namely, the energy, mass and linear momentum balances. In addition, there are often needed constitutive equations, which can include heat transfer and pressure drop correlations and thermodynamic fluid property relations.

Depending on the accuracy and computational time, dynamic models can be classified into two categories: data-driven and physics-based models [22]. The data-driven models are based on the knowledge of the system coming from measurements or previous simulations, and make use of computational methods such as machine learning [30] or transfer function identification to develop models of high computational efficiency [31]. The drawback is that the accuracy of the model is highly dependent on the quality of the data set [32]. Extrapolation out of the operating range of the data set can lead to poor accuracy and estimation errors. If there are modifications to the original system, the model cannot be adapted if physical information is missing. Physics-based models are component-level models based on the conservation laws (mass, energy and momentum). For this reason, changes in the system configuration and tests of the system performance in extreme operating conditions can be assessed more easily. The complexity of both data-driven and physics-based models can change according to the required accuracy and computational time. Low-order models are developed by doing several simplifications in physics-based models as well as by selecting a lower number of independent variables for data-driven models. They can be used for real-time applications and for longer time simulations, such as annual simulations. High-order models are suited for shorter time period simulations, spanning from a few minutes to several hours, when the computation time is not critical, and these are the ideal choice for the development of controllers of broader applicability.

A list is shown in Table 2 of the dynamic modeling studies of ORC systems and the applied modeling approaches.

Table 2: List of dynamic modeling studies in the area of organic Rankine cycle technology.

Ref.	Application	Software	Cycle		Modeling approach			
			Configuration	Working fluid	Evap.	Cond.	Pump	Exp.
[28]	WHR (ICE)	gPROMS	Basic	Ethanol	MB	MB	η_{is}	η_{is}
[33]	Solar	Matlab/Simulink	Basic	R245fa	FV	FV	η_{is}	η_{is}
[34]	Solar	Matlab/Simulink	Basic	R245fa	MB	MB	η_{is}	η_{is}
[35]	WHR (ICE)	Matlab/Simulink	Dual evap.	R245fa	FV	FV	Pr. Map	Pr. Map
[35]	WHR (ICE)	GT-POWER	Dual evap.	Ethanol	FV	FV	Pr. Map	Pr. Map
[29]	WHR (ICE)	Matlab/Simulink	Basic	14 Pure fluids	MB	MB	η_{is}	η_{is}
[36]	WHR (ICE)	Matlab/Simulink	Dual evap.	R245fa	MB	MB	Pr. Map	Pr. Map
[37]	WHR	Matlab/Simulink	Basic	R123	FV	FV	η_{is}	Pr. Map
[38]	WHR	Matlab/Simulink	Recuperated	R134a	MB	MB	Pr. Map	Pr. Map
[39]	WHR (ICE)	Matlab/Simulink	Dual evap.	Ethanol	MB	MB	Pr. Map	Pr. Map
[40]	WHR (ICE)	Matlab/Simulink	Basic	NA	MB	MB	η_{is}	η_{is}
[41]	WHR (ICE)	Modelica	Basic	R245fa	FV	FV	Pr. Map	Pr. Map
[42]	WHR (ICE)	LMS Imagine.Lab	Basic	Ethanol	FV	FV	Pr. Map	Pr. Map
[43]	WHR (ICE)	Matlab/Simulink	Dual loop	Toluene	MB	MB	η_{is}	η_{is}
[44]	WHR	Matlab/Simulink	Basic	NA	MB	MB	η_{is}	η_{is}
[45]	WHR (ICE)	NA	Basic	Acetone	FV	FV	Pr. Map	Pr. Map
[46]	WHR (ICE)	NA	Basic	R134a	MB	MB	η_{is}	η_{is}
[47]	WHR	Modelica	Recuperated	SES36	FV	FV	Pr. Map	Pr. Map
[31]	WHR (ICE)	NA	Basic	R245fa	MB	MB	η_{is}	η_{is}
[48]	WHR (ICE)	Matlab/Simulink	Dual evap.	Ethanol	MB	MB	NA	NA
[49]	Geothermal	VMGSim	Recuperated	n-Pentane	MB	MB	Pr. Map	Pr. Map
[50]	WHR (ICE)	Matlab/Simulink	Dual evap.	NA	FV	FV	η_{is}	η_{is}
[51]	WHR (ICE)	Matlab/Simulink	Basic	Ethanol	FV	FV	NA	NA
[52]	WHR (ICE)	NA	Recuperated	R245fa	FV	FV	η_{is}	η_{is}
[53]	WHR (ICE)	Modelica	Basic	NA	FV	FV	NA	NA
[54]	WHR	NA	Basic	NA	FV	FV	η_{is}	η_{is}
[55]	WHR	Matlab/Simulink	Basic	R245fa	FV	FV	NA	NA
[56]	WHR (ICE)	Matlab/Simulink	Dual evap.	Ethanol	FV	FV	η_{is}	η_{is}
[57]	WHR	Matlab/Simulink	Basic	R245fa	MB	MB	η_{is}	η_{is}
[58]	WHR (ICE)	Matlab/Simulink	Basic	Ethanol	MB	MB	η_{is}	η_{is}
[59]	WHR (ICE)	Matlab/Simulink	Basic	R245fa	MB	MB	η_{is}	η_{is}
[60]	WHR (ICE)	Matlab/Simulink	Basic	R245fa	MB	MB	η_{is}	η_{is}
[61]	WHR (ICE)	Matlab/Simulink	Basic	R123	FV	FV	η_{is}	η_{is}
[62]	Geothermal	Matlab/Simulink	Recuperated	R245fa	MB	MB	η_{is}	η_{is}
[63]	WHR (ICE)	Matlab/Simulink	Basic	Ethanol	MB	MB	NA	NA
[64]	WHR	Matlab/Simulink	Basic	R245fa	MB	MB	η_{is}	η_{is}
[65]	WHR (ICE)	Matlab/Simulink	Supercritical	R134a	FV	FV	η_{is}	η_{is}
[66]	WHR (ICE)	GT-Power	Basic	R245fa	FV	FV	η_{is}	η_{is}
[22]	WHR	Modelica	Basic	R245fa	FV	FV	Pr. Map	Pr. Map
[21]	WHR	Modelica	Basic	R245fa	MB	MB	Pr. Map	Pr. Map
[67]	WHR	Modelica	Basic	R245fa	FV	FV	Pr. Map	Pr. Map
[68]	Geothermal	VMGSim	Basic	NA	MB	MB	η_{is}	η_{is}
[69]	Geothermal	Modelica	Dual evap.	R245fa	TV	-	-	-

NA = not available; MB = moving boundary approach; FV = finite volume approach; TV = two-volume approach; Pr. Map = performance map; η_{is} = isentropic efficiency.

2.1 Heat exchangers

The dynamic response of the ORC system is mainly governed by the heat exchangers. The heat exchangers account for the majority of performance lag due to dynamic changes in the operating conditions. This is because the time constant of the heat exchangers is much larger than those of expanders and pumps, and mechanical transients are much faster than heat transfer phenomena. This is valid not only for ORC systems [22,23], but also for conventional thermal power generation plants [70]. For instance, Shin et al. [71] studied the response time of a gas-fired combined cycle power plant to rapid changes in the gas turbine load. As it can be seen in Figure 1, the gas turbine could reach stable operation in 4 s, whereas the steam generator required more than 200 s for the high pressure part and 2000 s for the low pressure part to reach steady operation.

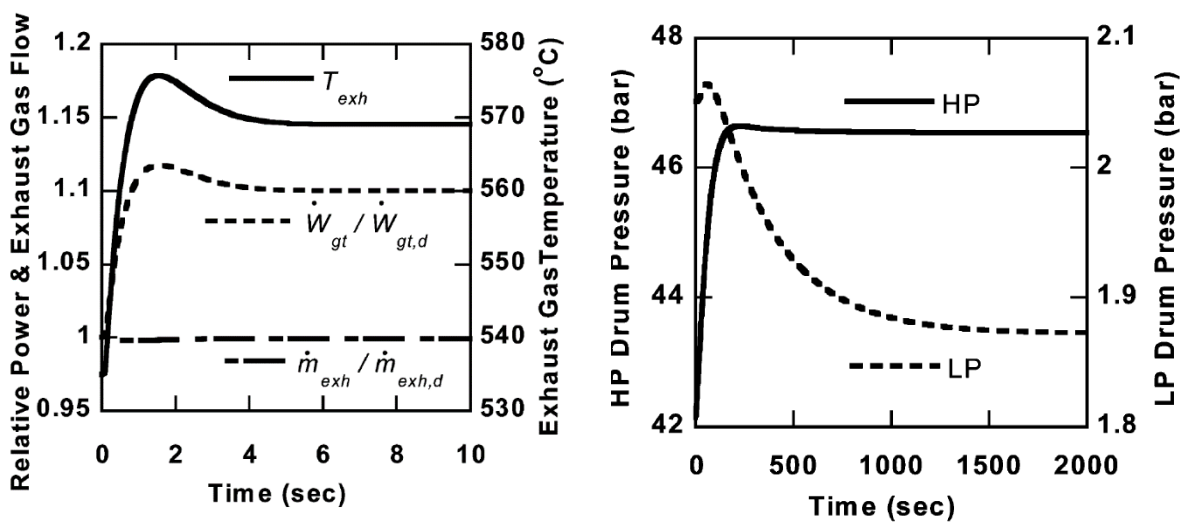


Figure 1: Time response of a) gas turbine and b) drum pressure of a gas-fired combined cycle power plant [71].

In the particular case of heat exchangers involving two-phase flows, two commonly adopted heat exchanger modeling approaches are the finite volume and the moving boundary methods. Both methods are based on the conservation laws of energy, mass and momentum for a defined control volume. A third modeling approach, based on two volumes in non-equilibrium, is also illustrated. The conservation equations required to model the heat exchanger are mass, momentum and energy balances for the heat source and working fluid.

2.1.1 Moving boundary method

In a moving boundary (MB) model, the fluid flow in the heat exchanger is divided into as many control volumes as states of matter of the working fluid (i.e., liquid, two-phase, vapor) in the fluid flow. The size of the control volumes varies in real time during transient operation, following the saturated liquid and the saturated vapor boundaries. A moving boundary model of an evaporator is shown in Figure 2. Solving a moving boundary model is a non-linear implicit problem that leads to convergence issues if proper guessed values are not provided [72].

The issues related to the guessed values decrease the robustness of the proposed models. The set of non-linear systems of equations of the MB is generally solved using the Newton solver [73]. However, the computational effort of the model depends on whether the system of the equations is presented in a causal formulation or an acausal formulation.

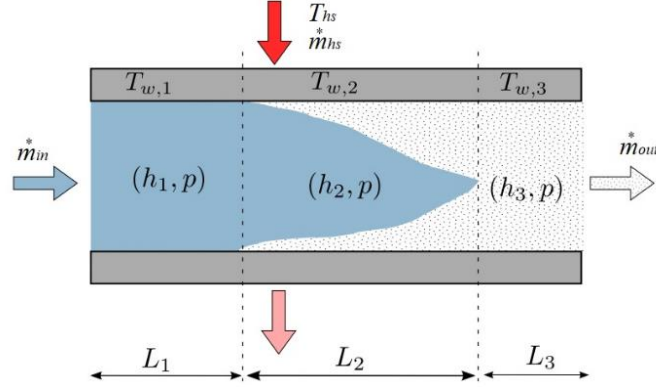


Figure 2: Moving boundary approach layout for the evaporator, Peralez et al. [31].

The mass balance of the working fluid is given by:

$$\frac{\partial(A_{wf,XA}\rho_{wf})}{\partial t} + \frac{\partial\dot{m}_{wf}}{\partial z} = 0 \quad (1)$$

Since there is no mass entering and leaving the wall, there is no need for a mass balance of the wall. Generally, the dynamics of the heat source are fast enough, leading the term $\frac{\partial\dot{m}_{hs}}{\partial z}$ to be close to zero. Therefore, it is not necessary to apply a mass balance for the heat source. The energy balance of the working fluid and exhaust gas share the same general form, given by:

$$\frac{\partial(A_{hs,XA}\rho h - pA_{hs,XA})}{\partial t} + \frac{\partial\dot{m}h}{\partial z} = \pi D_{eq}U(T_w - T_{wf}) = \pi D_{eq}U\Delta T \quad (2)$$

D_{eq} is the effective flow path diameter for either the working fluid and exhaust gas, U is the overall heat transfer coefficient, and ΔT is the temperature difference between the fluid (working fluid or exhaust gas) and the wall. The energy balance of the wall is given by:

$$A_{w,XA}c_{p,w}\rho_w L_w \frac{dT_w}{dt} = U_{wf,w}A_{wf,w}\Delta T_{wf,w} + \eta_\epsilon U_{hs,w}A_{hs,w}\Delta T_{hs,w} \quad (3)$$

where subscript w represents the wall, c_p is heat capacity, L_w is the length in the axial direction, $A_{w,XA}$ is the heat transfer area between working fluid and the wall, $U_{wf,w}$ is the heat transfer coefficient between working fluid and the wall, $\Delta T_{wf,w}$ is the temperature difference between the wall and the working fluid, η_ϵ is the heat exchanger efficiency multiplier, which accounts for heat loss to the environment, $A_{hs,w}$ is the heat transfer area between the exhaust gas and the wall, and $U_{hs,w}$ is the heat transfer coefficient between the exhaust gas and the wall.

The linear momentum balance is typically considered to be static, and if the pressure drop is neglected, the balance becomes trivial:

$$\frac{\partial p_{wf}}{\partial z} = 0 \quad (4)$$

Eq. (1), Eq. (2), Eq. (3) and Eq. (4) represent the generalized forms of the mass, energy and linear momentum balances of the heat exchangers. These equations need to be extended to the subcooled, two-phase, and superheated regions in the moving boundary model of the heat exchangers.

2.1.2 *Finite volume method*

In the finite volume method, the flow length of the heat exchanger is discretized into n cells in which the energy and mass conservation equations are applied. The fluid properties are assumed to vary only in the flow direction. The finite volume model of a heat exchanger is shown in Figure 3.

The properties of the fluid for each volume can be calculated either at the mean states of the two nodes (“central scheme”), or it can be assumed that the properties of the fluid for each volume are equal to the properties of the fluid leaving the volume (“upwind scheme”). If the fluid flows only in one direction, the upwind scheme is more robust. The central scheme is more computationally intensive than the upwind scheme, but it deals better with discontinuities in the case of flow reversal [74]. The properties of the fluid at the cell boundaries are represented by the symbol “*” in Figure 3. The area of cell, volume of cell, temperature and pressure at each node are given by:

$$A_i = \frac{A}{n}; \quad V_i = \frac{V}{n}; \quad i = 1, 2, 3 \dots \dots n \quad (5)$$

$$h_i = \frac{h_{i+1}^* + h_i^*}{2}; \quad T_i = \frac{T_{i+1}^* + T_i^*}{2}$$

The mass balance for each cell and side of the heat exchanger is given by:

$$\frac{dm_i}{dt} = V_i \frac{d\rho_i}{dt} = \dot{m}_i^* - \dot{m}_{i-1}^* \quad (6)$$

$$\frac{dm_i}{dt} = V_i \left[\left. \frac{\partial \rho}{\partial h_i} \right|_p \frac{dh_i}{dt} + \left. \frac{\partial \rho}{\partial p_i} \right|_h \frac{dp_i}{dt} \right] = \dot{m}_i^* - \dot{m}_{i-1}^*$$

The energy balance is given by:

$$\frac{dU_i}{dt} = (\dot{m}_{i-1}^* h_{i-1}^* - \dot{m}_i^* h_i^*) + \dot{Q}_i \quad (7)$$

$$V_i \rho_i \frac{dh_i}{dt} = \dot{m}_{i-1}^* (h_{i-1}^* - h_{i-1}) - \dot{m}_i^* (h_i^* - h_i) + \dot{Q}_i + p_i \frac{dV_i}{dt}$$

The linear momentum balance is typically assumed to be static, and if the contribution of friction, buoyancy forces and fluid acceleration are considered, the balance becomes:

$$\frac{\partial p_{wf}}{\partial z} = \left(\frac{dp_{wf}}{dz} \right)_f + \left(\frac{dp_{wf}}{dz} \right)_b + \left(\frac{dp_{wf}}{dz} \right)_{acc} \quad (8)$$

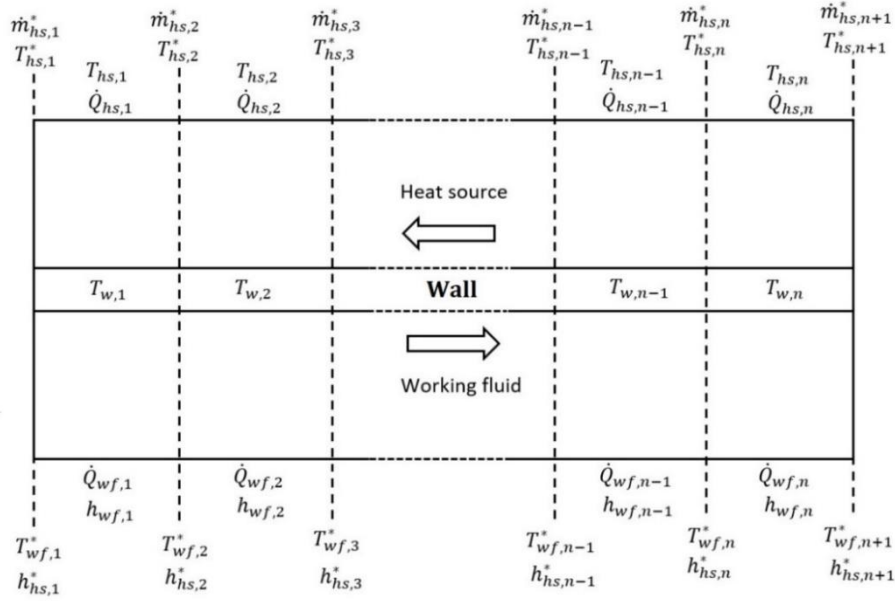


Figure 3: Finite volume modeling approach of the heat exchanger, adapted from Xu et al. [75].

2.1.3 Comparison of moving boundary and finite volume method

For a dynamic simulation of the ORC system, Wei et al. [21] compared the moving boundary and discretization technique approach. Their results suggested that both approaches can predict the dynamic performance of the ORC system fairly well, with less than 4 % relative difference compared with the experimental results. The simulation does not show the numerical chattering or oscillations in the results. As for the FV model, the level of discretization plays a critical role in the accuracy, computational effort and numerical inconsistencies.

As a general rule of thumb, a minimum number of 20 nodes is recommended to avoid numerical inconsistency in the simulation results [76]. The level of discretization might affect the working fluid phase boundary from one cell to the next, which would generate a numerical mass flow rate due to the discontinuity characterizing the density in the regions around the saturation lines [77]. Desideri et al. [76] developed a dynamic model of an ORC system based on FV models for the evaporator and condenser, and compared the accuracy of the expander power output for different levels of discretization and corresponding computational effort; see Figure 4.

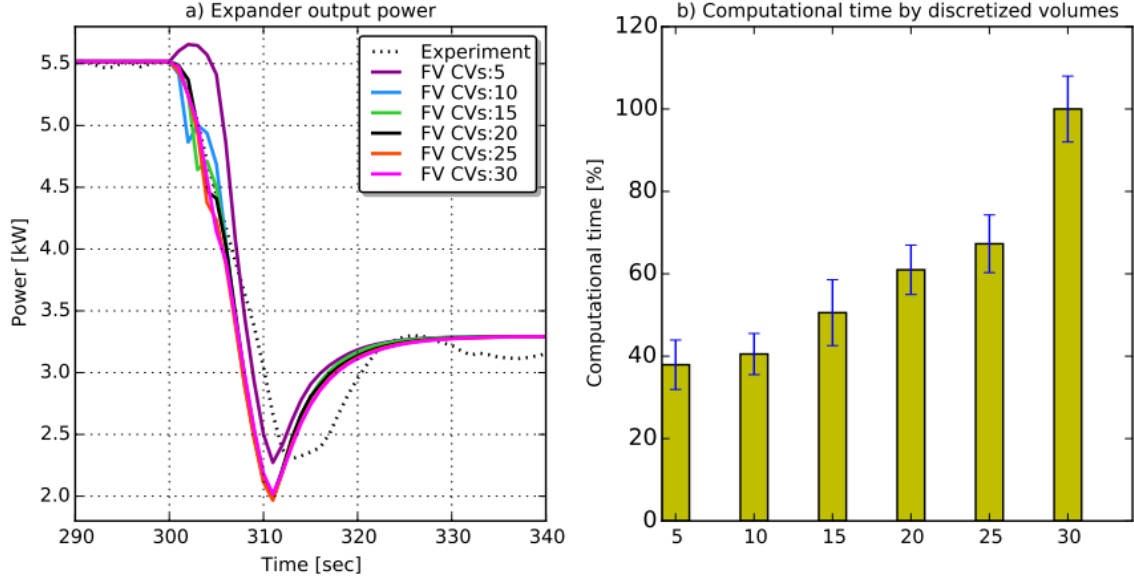


Figure 4: a) Expander output power as predicted by the finite volume model for different discretization levels. b) Computational time for the different discretization levels, Desideri et al. [76].

Applying a high level of discretization results in a better accuracy, but at the expense of a higher computation effort. For a number of CVs below 20, a non-physical oscillation between time $t = 300$ s and $t = 310$ s characterizes the expander output power simulation results. This phenomenon is explained by the displacement of the working fluid phase boundary from one cell to the next. This generates a numerical mass flow rate due to the discontinuity characterizing the density in the regions around the saturation lines. Increasing the number of CVs allows one to reduce the magnitude of this phenomenon. For a level of discretization above 20 CVs, negligible differences in the simulation results are registered, while the computational time of the models increases significantly, as shown in Figure 4b. This analysis allows one to identify a level of discretization of 20 CVs as a good compromise between accuracy and simulation speed for this specific simulation.

Although the heat transfer and pressure drop correlations provide accurate assessments of the heat transfer and pressure drop, it is generally difficult to use these correlations for dynamic simulations as they may slow down the calculation process, and potentially cause numerical instabilities and simulation failure. Quoilin et al. [78] proposed a fast, robust approach to model heat transfer. At nominal conditions, the heat transfer coefficient is determined and termed as the nominal heat transfer coefficient. For situations other than nominal conditions, the heat transfer coefficient is computed as follows:

$$\alpha = \alpha_n \left(\frac{\dot{m}}{\dot{m}_n} \right)^m \quad (9)$$

α and α_n are the heat transfer coefficient at the given state and the nominal heat transfer coefficient, \dot{m} and \dot{m}_n are the mass flow rate of working fluid at the given state and the nominal mass flow rate, and m is a constant that depends on the heat transfer correlation.

The heat transfer coefficient can also be calculated using Eq. (10) [78]. The transitions between the different heat transfer coefficients (liquid, two phase, and vapour) may cause inconsistency and simulation failure. The non-zero quality, x , width based transition by interpolating between the heat transfer coefficients can resolve this issue. In the interpolation function, the heat coefficients are represented in the form of vapor quality, x . The vapor quality is defined by an enthalpy ratio as presented in Eq. (10). This results in a smooth function as the vapor quality and its first derivative are continuous. This continuity avoids negative effects in the solution process.

$$\alpha = \begin{cases} \alpha_{liq} & \text{if } x < -\Delta x/2 \\ \alpha_{liq} + \frac{(\alpha_{tp} - \alpha_{liq})}{2} \cdot \left(\frac{1 + \sin(\pi x / \Delta x)}{2} \right) & \text{if } -\Delta x/2 < x < \Delta x/2 \\ \alpha_{tp} & \text{if } \Delta x/2 < x < 1 - \Delta x/2 \\ \alpha_{tp} + \frac{(\alpha_{vp} - \alpha_{tp})}{2} \cdot \left(\frac{1 + \sin(\pi(x-1) / \Delta x)}{2} \right) & \text{if } 1 - \Delta x/2 < x < 1 + \Delta x/2 \\ \alpha_{vp} & \text{if } x \geq 1 + \Delta x/2 \end{cases} \quad (10)$$

$$x = \frac{h - h_l}{h_l - h_v}$$

Desideri et al. [79] compared the FV and MB models based on experimental data. The heat transfer coefficients were calculated using Eq. (2), a heat transfer correlation, and a constant value of the heat transfer coefficient, respectively. The FV model predicts the experimental data more accurately than the MB, but with larger computational effort, as shown in Figure 5.

The transient of the pressure dynamic is very fast. This leads to stiff models, which necessitate small time steps that can increase dramatically the simulation time. Therefore, in most of the studies in the area of dynamic modeling of heat exchangers of ORC systems, the pressure drop is generally neglected or lumped into a single parameter. Wei et al. [21] assumed a linear pressure drop across the entire evaporator during dynamic modeling of the ORC system, while Xu et al. [75] included a pressure drop for each working fluid phase independently by assigning each phase its own linear pressure drop along the spatial length in the dynamic modeling of an ORC system.

The heat exchanger dynamic modeling is typically limited to one-dimensional modeling approaches, since two and three-dimensional spatial models bring a level of computational and analytical complexity that is unsuitable for the purposes of multi-component dynamic modeling and control.

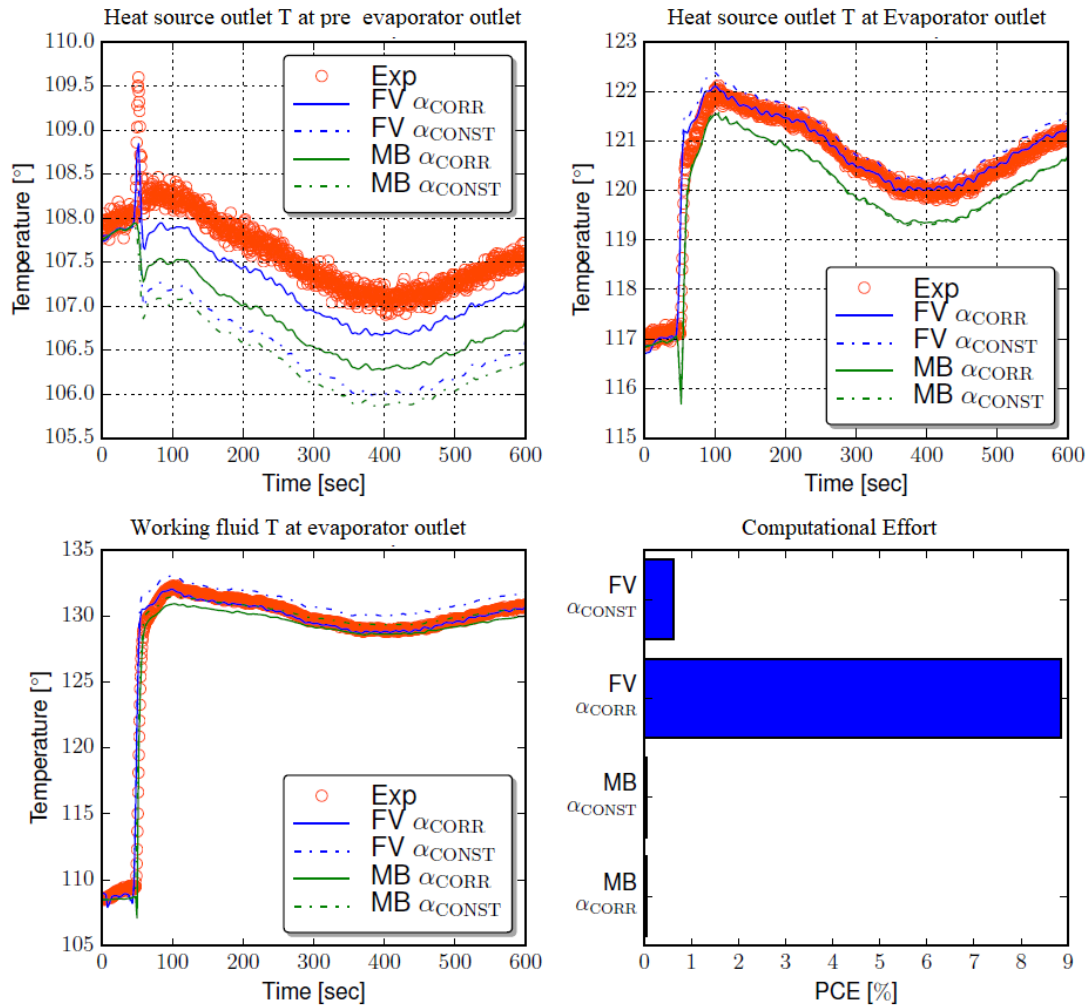


Figure 5: Results of the heat transfer coefficient analysis on the finite volume and moving boundary models, Desideri et al. [79].

The moving boundary modeling approach is much faster (by approximately three times) than the finite volume approach. However, the moving boundary approach has a lower accuracy than the finite volume approach when compared with experimental data. In addition, the moving boundary approach is more difficult to implement due to the complexity of variable control volume lengths, the need to incorporate the mean void fraction and the difficulty to extend the model to various heat exchanger types and geometries. The finite volume approach is simple, easy to derive, and easy to implement with various heat exchanger types and geometries due to the ease in reconfiguration of the model.

Furthermore, the finite volume method can provide additional values of the heat exchanger parameters, while the moving boundary method only provides values for the outlet of the component and lumped values. For example, the finite volume approach can provide the tube wall temperature at uniform length intervals along the length of the tube, while the moving boundary model only provides the lumped value for each working fluid phase.

Refer to Table 2 for the list of modelling methods applied to ORC systems.

2.1.4 Two-volume method

For phase-change heat exchangers, where evaporation or condensation occurs in the shell side of the heat exchanger, it might be advantageous to model the shell side considering only two volumes, liquid and vapor, which are not in thermal equilibrium, as shown in Figure 6. The interface between the two volumes defines the level of liquid in the shell. This model is suitable for kettle reboilers, which are used to vaporize the working fluid in large-scale ORC units [69], or shell-and-tube condensers with hot-well, where the liquid is collected at the bottom of the shell [80]. Depending on the evaporation and condensation rate in each of the volumes, mass is exchanged between the two volumes. The heat source or cold sink flow in the tube bundle, which can instead be discretized using a finite volume approach. The mass, energy and linear momentum balance of the liquid ('l') and vapor volumes ('v') are:

$$\begin{aligned}\frac{dm_l}{dt} &= \rho_l \frac{dV_l}{dt} + V_l \frac{d\rho_l}{dt} = \dot{m}_{cond}^* - \dot{m}_{evap}^* + \dot{m}_{in}^* \\ \frac{dm_v}{dt} &= \rho_v \frac{dV_v}{dt} + V_v \frac{d\rho_v}{dt} = -\dot{m}_{cond}^* + \dot{m}_{evap}^* - \dot{m}_{out}^* \\ \frac{d\rho_l}{dt} &= \left. \frac{\partial \rho_l}{\partial p_l} \right|_h \frac{dp_l}{dt} + \left. \frac{\partial \rho_l}{\partial h_l} \right|_p \frac{dh_l}{dt} \\ \frac{d\rho_v}{dt} &= \left. \frac{\partial \rho_v}{\partial p_v} \right|_h \frac{dp_v}{dt} + \left. \frac{\partial \rho_v}{\partial h_v} \right|_p \frac{dh_v}{dt}\end{aligned}\tag{11}$$

$$\begin{aligned}\dot{m}_{evap}^* &= \begin{cases} C_{evap} m_l (x_l - x_{l,ref}) & \text{if } x_l > x_{l,ref} \\ 0 & \text{elsewhere} \end{cases} \\ \dot{m}_{cond}^* &= \begin{cases} C_{cond} m_v (x_{v,ref} - x_v) & \text{if } x_v < x_{v,ref} \\ 0 & \text{elsewhere} \end{cases}\end{aligned}\tag{12}$$

$$p_{in}^* - \Delta p_{drop,in} = \rho_l g l_l + p_v$$

$$p_l = \frac{p_{in}^* - \Delta p_{drop,in} + p_v}{2}\tag{13}$$

$$p_v - \Delta p_{drop,out} = p_{out}^*$$

$$\begin{aligned}\frac{dU_l}{dt} &= \dot{m}_{in}^* h_{in}^* + \dot{m}_{cond}^* h_{sat,v} - \dot{m}_{evap}^* h_{sat,l} + \sum \dot{Q}_l \\ \frac{dU_v}{dt} &= -\dot{m}_{cond}^* h_{sat,v} + \dot{m}_{evap}^* h_{sat,l} - \dot{m}_{out}^* h_{out}^* + \sum \dot{Q}_v\end{aligned}\tag{14}$$

Eq. (12) defines the mass exchanged between the two volumes, i.e., the evaporation and condensation rates \dot{m}_{evap}^* and \dot{m}_{cond}^* . They depend on the two coefficients C_{evap} and C_{cond} , which can be tuned from experimental data, and on the vapor quality of the volumes x_l and x_v with respect to the references $x_{l,ref}$ and $x_{v,ref}$, which are ideally 0 and 1, respectively. $\Delta p_{drop,in}$ and $\Delta p_{drop,out}$ refer to the working fluid pressure drops at the inlet and outlet ports, where as $\rho_l g l_l$ is the geodetic pressure for the liquid volume.

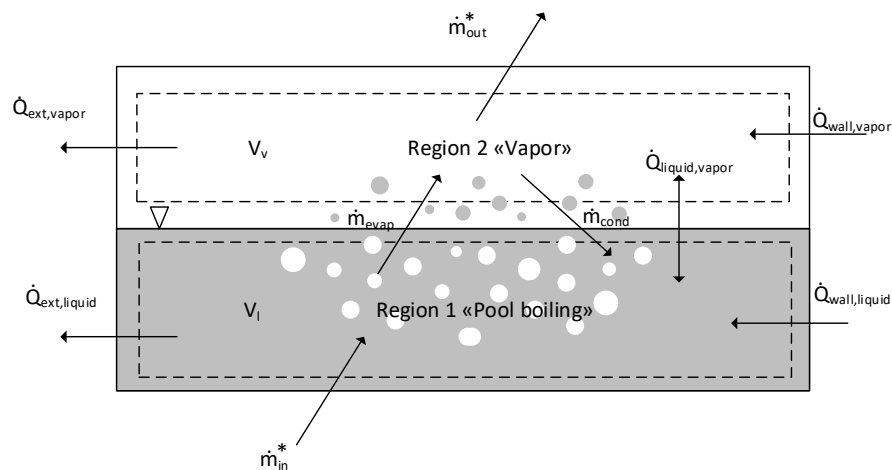


Figure 6: Two-volume model of the kettle reboiler, adopted from Pili et al. [69].

2.1.5 Numerical issues and mitigation strategies

The dynamic modeling is subject to different numerical issues, leading to potentially slow simulation or to simulation failures that can make the model unusable for some externally imposed operating conditions.

In the moving boundary method, the simulation issues generally arise when the iteration process leads the solver to evaluate a physically impossible solution (typically the temperature profile of hot and cold streams crossing along the length of the heat exchanger). This can be due to the heat exchanger model itself, or to the external models imposing impossible operating conditions on the heat exchanger.

Discontinuities in the model variables result in the phenomenon of chattering, a well-known issue in finite-volume, two-phase flow models. The chattering can lead the computed variables of the model to exceed their acceptable boundaries and cause failure of the simulation.

Failure in the dynamic simulations may occur during the initialization phase or during the simulation phase of heat exchangers involving a discretized modeling approach. If start and initial values are not assigned properly, the solver may set these variables to default values, leading to non-convergence of the heat exchanger model [78]. However, also with adequate start and initial values, the non-linear system might fail to converge during initialization. Li et al. [81] proposed a simple approach to improve the convergence of non-linear systems. During initialization, the heat transfer coefficients and pressure drops are assumed constant, and after a few seconds (once the system is stabilized), the pressure drop and heat transfer equations are activated one by one. Another key element in non-convergence of the simulation may be the result of zero mass flow rate in components, leading to a stiff system of equations, which may require a very small time step and consequently, the computation time may drastically increase. In order to work around the problem, a very small mass flow rate (non-zero) may be imposed, ensuring that the system of equations converges without affecting the results.

In order to avoid freezing of the simulations at the initiation of the disturbance, the disturbances should not be defined as a step change, but rather as smooth transitions, avoiding infinite derivatives in the components of the system.

Due to discontinuities in the model variables, chattering may occur and result either in simulation failure, extremely slow simulation or most often high-frequency oscillations. During the phase transition (liquid to two-phase) in two-phase heat exchanger models, a discontinuity in the first derivative of the density may lead to such issues. The simulation may fail or result in a stiff system if the cell-generated (and purely numerical) flow rate due to this discontinuity causes a flow reversal in one of the nodes as well as oscillations in pressure. Quoilin et al. [77] carried out a comprehensive analysis of the issues linked to simulation failures during integration in finite-volume flow models and provided several methods to tackle chattering and flow reversal problems. A filtering method, truncation method, smoothing of the density function and density derivative, a mean densities method, an enthalpy limiter method, and a smooth reversal enthalpy method were suggested to tackle such simulation failures and resolve these issues [77].

2.2 Expander

For the dynamic modeling of ORC systems, the time constants characterizing the expansion and compression processes are small compared to those of the heat exchangers. Thus, the models for the expansion machine can be based on empirical or semi-empirical algebraic correlations where dynamics are neglected, i.e., a lumped model based on performance curves or the semi-empirical model developed by Lemort et al. [82].

There are two types of expansion machines for ORC systems, the volumetric expander and the turbo-expander. The choice of the type of expander is dependent on the system design, size, and application. Since the residence time of the working fluid in the expander is relatively small in comparison to those of the evaporator and condenser, the use of a static model is preferred for the modeling of the expansion machine. The model of the expander should include both the first and second thermodynamic laws. The first law includes the dependencies among pressure, flow rate, and rotational speed, while the second law relates the isentropic efficiency with the flow rate and pressure as well as the rotational speed [83].

2.2.1 Volumetric expander

The dynamics of the expander and the pump are very fast compared to those of the evaporator and condenser and are modeled at steady-state. Neglecting the heat loss, a volumetric expander can be modeled by its isentropic efficiency and filling factor, given by:

$$\eta_{exp,is} = \frac{\dot{W}_{exp}}{\dot{m}_{wf}(h_{exp,in} - h_{exp,out})} \quad (15)$$

$$\phi = \frac{\dot{m}_{wf}}{\rho_{exp,in} V_{sw} N_{exp}} \quad (16)$$

The outlet enthalpy is given by:

$$h_{exp,out} = h_{exp,in} - \eta_{exp,is}(h_{exp,in} - h_{exp,out,is}) \quad (17)$$

In the case that experimental data are available, a performance map of a volumetric expander can be obtained, predicting the isentropic efficiency as a function of the expander inlet pressure, expander rotational speed, and expander pressure ratio (see e.g. reference [47]). The mass flow rate through an expander is given by:

$$\dot{m}_{wf} = \phi \rho_{exp,in} V_{sw} N_{exp} \quad (18)$$

The losses of volumetric expanders include leakage losses, under- and over-expansion losses, friction losses, and heat losses. In order to obtain an accurate result, the work done by a volumetric expander should be calculated considering both the under-expansion and over-expansion losses [22,57]. Quoilin et al. [84] presented a detailed semi-empirical model of a scroll expander, accounting for heat losses, working fluid leakage loss, and under-expansion and over-expansion losses. The model is based on the physics of the expansion process across the machine, where a few unknown parameters are tuned by fitting with experimental data.

2.2.2 Turbo-expander

The dynamic of the turbine is very fast compared to that of the heat exchangers, and thus the turbine model is at steady-state. A performance map of the turbine can be used to calculate the mass flow rate through the turbine as a function of the rotational speed and pressure ratio:

$$\dot{m}_{wf} = \text{performance map}(N_{exp}, p_{in,exp}) \quad (19)$$

Xu et al. [75] used the turbine inlet temperature and Wei et al. [21] used the pressure ratio from the turbine performance map to calculate the mass flow rate through the turbine. The semi-empirical formulation of the Stodola equation [85] can be used to calculate the mass flow rate of the working fluid through the turbine:

$$\begin{aligned} \dot{m}_{wf,exp} &= K_{eq} \sqrt{\rho_{in,exp} p_{in,exp} (1 - (PR)^{-2})} \\ PR &= \frac{p_{in,exp}}{p_{out,exp}} \end{aligned} \quad (20)$$

The K_{eq} integrates the equivalent inlet nozzle cross-section and the discharge coefficient and is calculated from the turbine performance at the nominal condition:

$$K_{eq} = \frac{(\dot{m}_{wf,exp})_n}{\sqrt{(\rho_{in,exp})_n (p_{in,exp})_n [1 - (PR_n)^{-2}]}} \quad (21)$$

The enthalpy at the outlet of the turbine is given by:

$$h_{out,exp} = h_{in,exp} - \eta_{exp,is}(h_{in,exp} - h_{out,is,exp}) \quad (22)$$

In most of the previous studies, the isentropic efficiency of the turbine was assumed constant. However, since the ORC system mostly operates far from design point in transient conditions, assuming a constant isentropic efficiency may lead to significant errors in the dynamic response of the ORC system [83]. Also the part-load performance in steady-state conditions will be inaccurately predicted by assuming a constant isentropic efficiency of the expander. An alternative to assuming a constant is to obtain the turbine isentropic efficiency from a turbine performance map, as in e.g. Xu et al. [75]:

$$\eta_{exp,is} = \text{performance map}(N_{exp}, PR_{exp}, T_{in,exp}) \quad (23)$$

The power output of the expander is given by:

$$\dot{W}_{exp} = \dot{m}_{wf}(h_{in,exp} - h_{out,exp}) \quad (24)$$

2.3 Pump

The dynamic response of the working fluid pump is very fast compared to that of the heat exchangers; hence, the pump is typically modeled using a steady-state lumped parameter model [60]. Such model can be based on performance maps provided by the pump manufacturer. The performance chart includes head versus volume flow curves at different rotational speeds. If the map is provided with one rotational speed only, curves at other speeds can be approximated by means of a kinematic similarity principle. Another type of performance chart includes efficiency curves on the head-flow plane or in terms of power consumption curves as a function of flow and speed [83]. Heat losses to the environment are usually neglected.

For centrifugal pumps, the volume flow rate is a function of both the head and the rotational speed. The crossing point between the characteristic curve of the system and the performance curve of the pump defines the operating point, as shown in Figure 7.

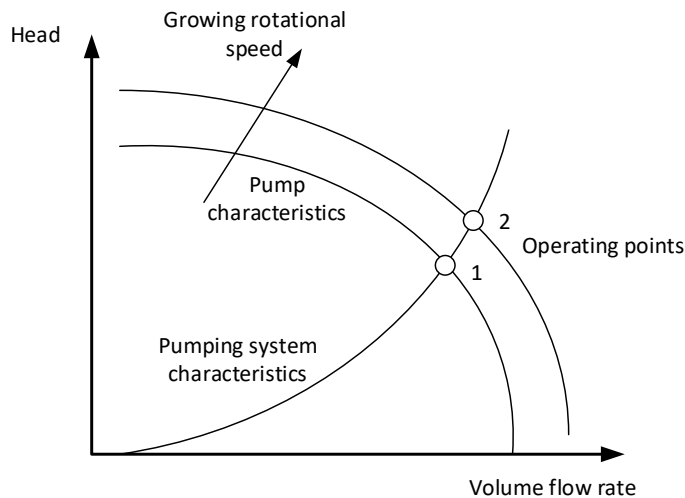


Figure 7: Flow-head characteristics of a centrifugal pump.

For a positive-displacement pump, the mass flow rate through the working fluid pump is obtained from the performance curve (pump speed vs mass flow rate). If the dependency on the pressure ratio is neglected:

$$\begin{aligned}\dot{m}_{wf,pu} &= \text{performance map}(N_{pu}) \\ \dot{m}_{wf,pu} &= C + C_1 f_{pu}\end{aligned}\quad (25)$$

where N_{pu} is the pump speed, C and C_1 are empirical constants, and f_{pu} is the frequency of the pump motor. In case the performance maps are not available, the mass flow rate can be obtained from the volumetric efficiency of the pump:

$$\dot{m}_{wf} = \dot{m}_{wf,ideal} \eta_{vol,pu} \quad (26)$$

The volumetric efficiency, $\eta_{vol,pu}$, is a function of the pump speed ω_{pump} (revolutions per second) and the pressure ratio across the pump [56]. The ideal mass flow rate of the pump is given by:

$$\dot{m}_{wf,ideal} = V_{pd} \rho N_{pu} \quad (27)$$

V_{pd} is the pump displacement volume, and ρ is the working fluid density. The pump power consumption and the outlet temperature are given by:

$$\dot{W}_{pu} = \frac{\dot{m}_{wf} (p_{out,pu} - p_{in,pu})}{\rho \eta_{is,pu}} \quad (28)$$

$$T_{out,pu} = T_{in,pu} + \frac{(1 - \eta_{is,pu})}{\dot{m}_{wf,pu} C_{p,pu}} \dot{W}_{pu} \quad (29)$$

The isentropic efficiency can also be expressed as a function of known parameters (polynomial fit) from the performance map of the pump provided by the manufacturer. These parameters may include the pump capacity fraction, $X_{pu,cf}$, defined by a reference [86].

$$X_{pu,cf} = \frac{v_{in,pu} \dot{m}_{wf,pu}}{\dot{V}_{in,pu,max}} \quad (30)$$

Depending on the size of the pump, the pump capacity factor is limited by the boundary condition, $\dot{V}_{su,pu,min} \leq X_{pu,cf} \leq 1$. The known parameters in the polynomial fit can be represented by the mass flow rate fraction, $X_{pu,mf}$, given by [75]:

$$X_{pu,mf} = \frac{\dot{m}_{wf,pu}}{\dot{m}_{wf,pu,max}} \quad (31)$$

$\dot{m}_{wf,pu}$ is mass flow rate at any given condition while $\dot{m}_{wf,pu,max}$ is maximum mass flow rate that pump can deliver. Desideri et al. [79] used a second-order polynomial, as a function of the non-dimensional pressure ratio and non-dimensional pump frequency, to estimate the isentropic efficiency of the pump:

$$\eta_{pu,is} = C + C_1 f_{pu} + C_1 (f_{pu})^2 + C_3 r_{pu} + C_4 (r_{pu})^2 + C_5 f_{pu} r_{pu} \quad (32)$$

In most of the simulation studies, the isentropic efficiency of the pump is assumed to be between 60 % and 85 %. However, a review of the experimental data obtained for ORC systems indicates that the isentropic efficiency of the pump can be as low as 40 % [16]. As with the expander, assuming a constant isentropic efficiency may lead to inaccurate dynamic response or part-load predictions; however, in this regard the influence of the pump is less than that of the expander. This is because the pump power is usually lower than 10 % of the mechanical power at the turbine shaft.

Refer to table 2 for the list of studies presenting performance estimation for pump and expander models.

2.4 Storage tank/Liquid receiver

During the transient operation of the ORC system, the reservoir/storage tank acts as a buffer for the working fluid. The amount of working fluid charge and leakage can significantly alter the ORC system dynamics. A system with over filled working fluid will lead to conditions, where the working fluid start accumulating in the condenser as liquid. This will result in a larger degree of sub-cooling and a higher condenser pressure resulting in reduced power output and decreased efficiency.

The storage tank avoids the accumulation of working fluid in the condenser. On the other hand, if the working fluid amount is too small or working fluid has leaked out of the system, the system start-up will become almost impossible because during the start-up phase the pump will run out of working fluid and a cyclic flow may not be established. For the modelling of the storage tank (liquid receiver), it is usually assumed that the liquid and vapor phases are in thermodynamic equilibrium at all times, i.e., the vapor and liquid are assumed saturated at the given pressure. The pressure drop is typically neglected. The mass balance is given by:

$$\frac{d\dot{m}_{wf}}{dt} = \dot{m}_{in,wf} - \dot{m}_{out,wf} \quad ; \quad \frac{d\dot{m}_{wf}}{dt} = V \cdot \left[\left. \frac{\partial \rho}{\partial h} \right|_p \cdot \frac{dh}{dt} + \left. \frac{\partial \rho}{\partial p} \right|_h \cdot \frac{dp}{dt} \right] \quad (33)$$

V is the volume of the liquid receiver tank in m^3 . The density of the liquid can be represented in terms of a liquid level fraction L (0 when the tank has only vapor, 1 when the tank is full of liquid), given by:

$$\rho = \rho_l Y + (1 - Y)\rho_v \quad (34)$$

The term, Y , is the level of saturated liquid in the receiver tank of the ORC system. Inserting the equation for the density, Eq. (34), into the mass balance equation, Eq. (33), gives the following equation:

$$V \left[(\rho_l - \rho_v) \cdot \frac{dY}{dt} + \left(\frac{d\rho_l}{dt} \cdot Y + \frac{d\rho_v}{dt} \cdot (1 - Y) \right) \right] = \dot{m}_{in,wf} - \dot{m}_{out,wf} \quad (35)$$

The generalized relation for the energy balance for the receiver tank [79] is given by:

$$\rho h = Y\rho_l h_l + (1 - Y)\rho_v h_v \quad (36)$$

Substituting Eq. (36) into Eq. (7), the mass balance in receiver tank can be represented as [79]:

$$V \left\{ \frac{dY}{dt} (h_l \rho_l - \rho_v h_v) + \frac{dp}{dt} \left[Y \cdot \left(h_l \frac{d\rho_l}{dp} + \rho_l \frac{dh_l}{dp} \right) + (1 - Y) \cdot \left(h_v \frac{d\rho_v}{dp} + \rho_v \frac{dh_v}{dp} \right) - 1 \right] \right\} \quad (37)$$

$$= \dot{m}_{in,wf} h_{in} - \dot{m}_{out,wf} h_{out}$$

Another aspect of ORC system design is to avoid that the change in the level/height of the receiver tank, at any time during operation, leads to a reduction of the net positive suction head available, becoming lower than net positive suction head required by the pump. Based on the level of working fluid in the receiver tank, the loss/leakage of working fluid charge quantity can be identified and working fluid quantity can be replenished.

2.5 Control valves

The dynamic characteristics of the control valve can be modeled with relevant equations that correlate the valve opening, boundary conditions and the flow through the component. The control valve model for WHR-based ORC systems is based on either the incompressible flow for liquid flow or the compressible flow for vapor and two-phase flow [56]. If the system dynamics are fast, the valve positioning servo-system plays an important role in determining the closed-loop dynamic behavior of the system and should be included in the model [83]. However, it is difficult to gain access to information about the servo-positioner dynamics; hence, first-order or second-order linear systems can be used to consider these dynamics.

In case experimental data are available for the ORC system, an empirical correlation can be developed to calculate the mass flow rate for incompressible flow based on the relative valve openings. Xu et al. [75] used an empirical approach to estimate the incompressible flow rate through the control valve for a parallel evaporator ORC system. In the parallel evaporator configuration, the waste heat from an internal combustion engine is recovered using two evaporators in a parallel arrangement, one recovers heat from the exhaust gas recirculation flow and the other from the exhaust gas tail pipe [75]. The mass flow rate for such configuration is given by:

$$\dot{m}_{wf} = \dot{m}_{wf,ev1} + \dot{m}_{wf,ev2} \quad (38)$$

$$r_{\dot{m}} = \frac{\dot{m}_{wf,ev1}}{\dot{m}_{wf,ev2}} \quad (39)$$

$$r_{\dot{m}} = C_d \left(\frac{\mu_{vl,1}}{\mu_{vl,2}} \right)^{c1} \quad (40)$$

$$\dot{m}_{wf,ev1} = \dot{m}_{wf} \left(\frac{r_{\dot{m}}}{r_{\dot{m}} + 1} \right) \quad (41)$$

$$\dot{m}_{wf,ev2} = \dot{m}_{wf} \left(\frac{1}{r_{\dot{m}} + 1} \right) \quad (42)$$

The parameters $\mu_{vl,1}$ and $\mu_{vl,2}$ are the opening of valves 1 and 2, respectively, before each evaporator. The discharge coefficient, C_d , and the constant $c1$ can be found by model identification [87]. The term, $r_{\dot{m}}$, is the mass flow rate ratio of the working fluid between the two evaporators. For cases where

experimental data are not available, the mass flow rate through the valve for incompressible flow can be determined as follows [56]:

$$\dot{m}_{cv} = \mu_{cv} C_d A_o \sqrt{2\rho(p_{in} - p_{out})} \quad (43)$$

The thermodynamic state of the working fluid at the outlet is calculated assuming an isenthalpic process through the valve. The mass flow rate through the valve for compressible flow is given by [75]:

$$\text{If } \left(\frac{2}{\gamma+1}\right)^{\frac{\gamma}{\gamma-1}} \leq \frac{p_{out}}{p_{in}} \leq 1 \quad (\text{subsonic}) \quad (44)$$

$$\dot{m}_{cv} = \mu_{cv} C_d A_o \sqrt{\frac{2\gamma}{\gamma-1} \rho_{in} p_{in} \left[\left(\frac{p_{out}}{p_{in}}\right)^{\frac{2}{\gamma}} - \left(\frac{p_{out}}{p_{in}}\right)^{\frac{\gamma+1}{\gamma}} \right]} \quad (45)$$

$$\text{If } 0 \leq \frac{p_{out}}{p_{in}} \leq \left(\frac{2}{\gamma+1}\right)^{\frac{\gamma}{\gamma-1}} \quad (\text{supersonic}) \quad (46)$$

$$\dot{m}_{cv} = \mu_{cv} C_d A_o \left(\frac{2}{\gamma+1}\right)^{\frac{\gamma+1}{2(\gamma-1)}} \sqrt{\gamma \rho_{in} p_{in}} \quad (47)$$

γ is the heat capacity ratio. Assuming an isentropic process across the valve, the outlet temperature can be estimated by the enthalpy and pressure at the outlet of the valve. There is only one previous study [46] that considered the internal structure of the servo valves to estimate the valve opening.

2.6 Sensors

The measuring instruments might have a significant delayed response, especially the temperature sensors [83]. If the time scale of the measuring instrument is not negligible compared to the closed loop response time, it should be included in the model. First or second-order, low-pass linear systems can be used for this purpose. Lemort et al. [53,88] modeled the delayed response of the pump actuator, temperature and pressure sensors by a first-order model with the help of the manufacturer data.

The dynamic modeling approach of the components of the ORC system are similar to conventional power plants such as combined cycle power plant [89–92], coal fired power plant [93–95], nuclear power plant [96–99], and concentrated solar power [100–102]. The dynamic modeling of these systems was carried in Dymola and Simulink. A comprehensive review of dynamic simulation, its development and application to various thermal power plants is presented in Ref. [70]. The underlying flow models and their fundamental assumptions and component level modeling of conventional thermal power plants are discussed in detailed.

3. Controller design

The choice of working fluid, thermodynamic design, and mechanical design of the ORC components are prerequisite for the controller development and are used as input data for the controller design. Initially, the specific and concrete goals of the control system should be defined in terms of control variables and suitable set points. The main tasks of the control system are to keep the system safe and stable, to minimize the impact of disturbances and to optimize the ORC operation. In order to avoid singularities in the trajectories of the system, the number of manipulated variables should be equal or higher than the number of control variables. In the most common case, they are chosen in equal number. In the next phase, the dynamic interactions among the manipulated variables and control variables are investigated by analyzing the dynamic response of the control variables to step changes or more generally rapid changes of the manipulated variables. The step responses and transfer functions can provide an insight to identifying the dominant time constants of the system, the fastest system variables, and the slowest system variables. The transfer functions can be developed from experimental data or simulations of a physics-based model. Transfer functions are algebraic equations based on an input-output relationship, whereas the physics-based models are ordinary differential equations described by means of inputs, outputs and states.

The basic control strategy of the ORC system can be divided into two basic approaches: following the connected load (FCL) and following the thermal energy input (FTE) [103]. The number of actuators which can be manipulated in the system, as well as the variables that need to be controlled and kept close to the set points, define the basic control strategy. For instance, the rotational speed of the expander can be kept constant or it can be varied according to the operating point for optimal part-load performance.

In the FCL mode, the expander and the generator are linked with the same shaft. A gearbox could be included to keep the same speed ratio between the expander and the generator, in the case they do not rotate at the same speed. In most cases, systems in FCL mode have the generator connected to the power grid without a power converter interface. The grid frequency and the number of poles of the stator winding of the generator determine the rotational speed of the generator (and the expander). The produced electric power from the generator needs to follow the variations of the electric demand, while the ORC process variables must be kept within safe operating limits. For this purpose, the heat source is controlled and adapted to the grid load. The FCL mode without a frequency converter is depicted in Figure 8.

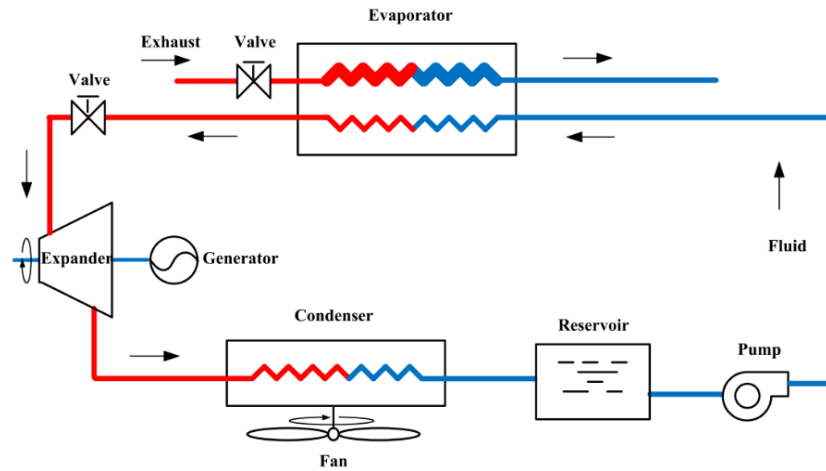


Figure 8: A schematic of the ORC system operating with the FCL mode, Zhang et al. [57].

If a frequency converter is included, the rotational speed of the expander can be used to control the upstream pressure of the expander, thus providing an additional degree of freedom. However, the operating conditions of the ORC system may change substantially due to changes in the load requirements or expander speed.

In the FTE mode, the goal of the system is to maximize the electricity production based on the heat available. The electric power from the generator follows the variations of heat source conditions. In an ideal case, all the heat available is fed to the ORC and converted into electricity. Some control elements on the heat source stream might still be required for extreme conditions to avoid overloading and/or thermal degradation of the working fluid. The FTE mode is shown in Figure 9. Here, a frequency converter is included, but if not present, the rotational speed of the expander is kept constant.

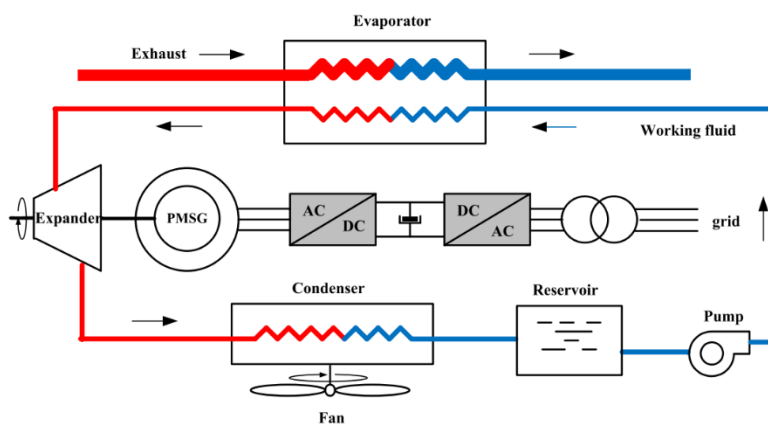


Figure 9: A schematic of the ORC system operating with the FTE mode, Zhang et al. [57].

In terms of a control strategy, the ORC system can be operated in the sliding pressure mode or the fixed pressure/variable mass flow mode, or a combination of both. However, these operational modes do not take into account the dynamic response of the ORC system. Nonetheless, they are useful for the part-load modeling of the ORC system and for defining the controller set points.

The sliding pressure control involves changes in the evaporator pressure resulting from the pump, evaporator and expander characteristics. The fixed pressured/variable mass flow rate scheme can be implemented by the addition of a pressure control valve (throttling valve) at the expander inlet to maintain pressure at a constant level in the evaporator, while the pump controls the mass flow rate through the cycle. This technique is easy to implement and might maintain a high-cycle efficiency (arguably theoretically) by keeping a high pressure at part-load; however, the throttling of the valve results in exergy losses, and the evaporation process is not optimized for the different heat source conditions (mismatches of the heat source and working fluid temperature lines in the T-Q diagram), resulting in pinch-point limitations and sub-optimal operation. The fixed pressure operation might be chosen at low load to ensure practical operation of the system, avoiding exceeding the minimal load of the components. For these reasons, at medium/nominal load range the sliding pressure mode is typically preferred. The operational strategy, which will then be important for the controller set points, can be optimized offline without accounting for the dynamics. If the dynamics is included, the controller requires an internal optimization function (or a supervisory block) that defines its actions by solving an online optimization problem.

As for the control of ORC systems, previous works were often carried out by validating a dynamic model against an open-loop response caused by a step disturbance or a set point change. The validated models are then simulated/tested with a control algorithm implemented in a closed loop. However, in practice the ORC system control schemes are highly dependent on the application, type of equipment and cycle configuration. The control scheme of a grid-connected unit is significantly different from that of a system in off-grid mode, because it can be assumed that larger plants in the grid will mainly be responsible for the stability of the grid in the first case, whereas in an off-grid system, the ORC unit has to ensure proper contribution to the frequency and voltage stability of the decentralized network. Renewable-based off-grid ORC systems have been proposed mainly for remote areas [104].

Various works utilizing validated dynamic models and discussing control schemes have been reported in the literature. Given the large amount of control ideas that have been proposed, a brief overview of the main classes of controllers is provided here. The main techniques are summarized in Figure 10.

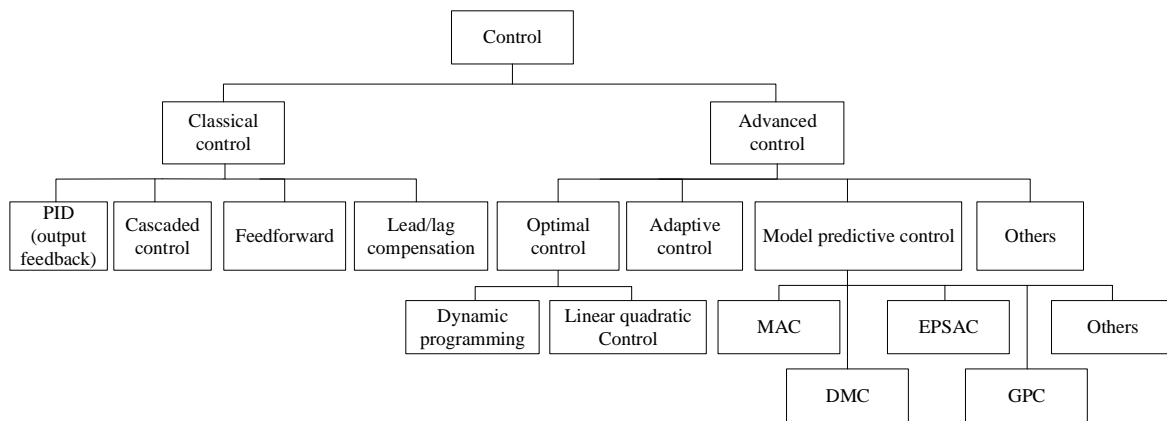


Figure 10: Overview of control techniques for ORC systems.

State-of-the-art ORC systems make use of proportional-integral-derivative (PID) controllers. These systems rely on the idea of directly acting on the error between the set point and the control variable (output feedback control) [105]. They have the advantage of being simple and easily available as electronic modules. The tuning of the controller parameters can be carried out empirically, directly on the plant without the need of a model. Some simple guidelines for controller tuning have been developed, such as the Ziegler-Nichols rules [106].

Another approach makes use of an input-output description of a linear or linearized dynamic model of the unit, and then applies techniques developed from the analysis of the linear dynamic system. For multi-variable systems, where more than a single pair input/output is considered, multiple PIDs that work independently of one another are typically installed. Given the interdependency of the system variables, for instance, between the evaporator pressure and the degree of superheating at the evaporator outlet, a conflict between the two controllers or performance degradation can occur. Some methods exist to decouple the controller action and avoid the interdependency among the variables, but the stringent mathematical conditions on the system properties that must be maintained limit the applicability of these methods. More measurements (not necessarily control variables) can be fed to the same controller, to increase the amount of information that it receives and improve its performance. This is the principle of cascaded control. Additionally, since linear systems do not account for internal time delays in the system, lead/lag compensators can be implemented to compensate for these phenomena. To conclude, another important improvement to classical PID controllers consists of including a feed-forward part acting on the manipulated variables. The feed-forward detects the disturbance or set point change and sets the manipulated variables to compensate directly for their impact before there is any noticeable change in the system output, which is different from what occurs in the case of classical PID controllers based on output feedback control.

In addition to the classical control techniques based on PID controllers, the improvements made in computational science have enhanced the development of advanced control methods, where the

controller makes use of the computational power of modern processors to design the controllers. Advanced controllers include optimal controllers (OC), adaptive controllers (AC) and model predictive controllers (MPC). Optimal controllers are designed to minimize a cost function (optimization target). Optimal control methods include dynamic programming (DP) and linear quadratic controllers (LQ). Both methods are based on a state-space model of the system, which gives information on the dynamics and time development of the system. Dynamic programming is a technique that defines future decisions based on the previous ones, operating in a recursive manner. The technique can be applied to both linear and non-linear systems, but in discrete form. DP has the advantage of allowing for real-time optimization of the controller set points. The main drawback is the computational effort required to solve the optimal problem, especially if the system has more than one state or control input [107].

LQ controllers are based on a state-space linear or linearized dynamic model of the system. They are a state-feedback technique and therefore require the knowledge of the system state. If not all the states are measurable, a state estimator (observer) has to be included to provide information on the system states. The design of LQ controllers is based on a trade-off between the performance of the controller to reach the desired state and the energy required to control the actuators. In fact, it can be worth accepting a penalty on controller performance, if this results in a reduction of its energy consumption or in an increased lifetime of the actuators. To reach this goal, a quadratic cost function is minimized to design the controller feedback matrix. LQ controllers can handle multi-variable systems with no particular increase in complexity. The drawback when applied to non-linear systems is that the technique was developed for linear systems and cannot account for the nonlinear couplings between the systems variables. LQ controllers cannot be used if the system states cannot be measured or estimated.

Such state estimators (observers) have been developed both for linear and non-linear systems, and they can be deterministic or stochastic. State estimators make use of the manipulated variables and measurable system outputs to estimate the system state. The separation principle allows for the design of the controller and the state estimator to be carried out separately. For linear systems, the Luenberger observer is used to minimize the error between the system state and the estimation. If stochastic noise is present in the system measurements and inputs, the linear Kalman filter should be preferred because it minimizes the sum of the estimation error variances. Non-linear state estimators have also been developed, but the computational effort increases significantly. The Extended Kalman Filter (EKF) and Unscented Kalman Filter (UKF) have proven to have good estimation capabilities. Both filters have similar computational effort, but the UKF has shown to have higher speed of convergence and to be more robust against uncertainties. Other state estimators exist, such as the particle filter and moving horizon estimators, but they require considerable computational effort.

If changes in the system occur over time or uncertainties are initially unknown, it would be ideal to use online adjustable controllers, which can react and adjust their parameters according to an estimation for the changes or uncertainties. These controllers are also known as adaptive controllers. There are many

different adaptive control techniques, varying from gain-scheduling, extremum-seeking and generalized predictive control. While having the advantage of being able to deal online with changes and uncertainties in the system, it might be difficult to obtain robust, high-performance controllers that work in the entire continuous range of the estimated parameters.

A further development in the 1980s regarded the introduction of Generalized Predictive Controllers (GPC). These controllers, which can also be considered as a subgroup of the family of the adaptive controllers, minimize a cost function where the controller bases the choice of the future inputs on the prediction of the system evolution in future time steps. To reach this goal, an identification model of the system is used, which relates inputs, outputs and disturbances. If the time horizon for the optimization is infinite, the GPC becomes equivalent to the LQ control.

Similar to the GPC, several other techniques have been developed which predict the response of the system to decide how to set future manipulated variables. These include Model Algorithmic Control (MAC), Dynamic Matrix Control (DMC), Extended Prediction Self Adaptive Control (EPSAC) and Predictive Function Control (PFC). All these algorithms are part of the family of Model Predictive Controllers (MPC). The advantage of MPCs is that they account for constraints on both the control and manipulated variables. The algorithms differ in the adopted process model (impulse response, step response, transfer functions, state-space, neural networks), in the objective function, and in the determination of the control law. Particular attention has been paid to MPC methods because of their main advantages [108]:

- They can be used in a large variety of systems, even more complex ones;
- Multiple variables can be considered with no particular increase in effort;
- They can handle constraints in the optimization of the control law.

If the target function includes minimization of costs or maximization of profits as well as the net power output, the term economic MPC is often used. Economic MPC can define controller optimal set points without previous offline optimization. As drawbacks for the entire MPC class, the derivation of the control law is more complex than for simple PID controllers, the control performance is largely affected by the quality of the model, and the computational power might be an issue, since an online optimization needs to be carried out each time step. The advantages and disadvantages of each control approach are presented in Table 3.

Table 3: Summary of control techniques for ORC systems.

Control technique	Model-based	Linear/Nonlinear	State estimator	Single/Multi-variable	Development effort	CPU effort	Performance
PID (empirical)	No	NA	No	Mostly single	+	+++	-
PID with linear system analysis	Yes	Linear	No	Mostly single	++	+++	-
Cascaded control	Yes	Linear/Nonlinear	No	Both	+	++	+
Feed-forward	Yes	Linear/Nonlinear	No	Both	+	+	+
Lead/lag compensation	Yes	Nonlinear	No	Mostly single	+	+++	+
Dynamic Programming	Yes	Linear/Nonlinear	Yes/No	Mostly single	--	--	+++
Linear Quadratic	Yes	Linear	Yes	Multi-variable	-	+	++
Adaptive	Yes	Linear/Nonlinear	Yes/No	Multi-variable	--	---	+++
MPC	Yes	Linear/Nonlinear	Yes/No	Multi-variable	--	---	++++

The ORC cycle layout and component selection also have an influence on the controllability of an ORC system [83]. For instance, an ORC system with controllable speed volumetric expander will have an additional parameter to control the evaporator pressure and thus allowing a tighter control, even with classical controllers [22]. ORC units with an intermediate heat transfer loops are easier to control due to the thermal inertia of the intermediate heat transfer loop and can therefore operate with classical controllers. The dynamics of recuperated ORC units is more damped compared to non-recuperated systems owing to the additional thermal inertia of the recuperator.

High temperature ORC units with compact heat exchangers are more susceptible to thermal shocks that may cause heat exchanger damage during an emergency shutdown. Overall, each system has a different dynamic behavior and might need different control strategies, governed by the process dynamics and the application requirements.

3.1 Proportional-integral-derivative control

The simplest control to guarantee stability of an ORC unit, is to have a PI controller that manipulates the speed of the pump to keep the liquid level in the receiver tank constant. In this way, the ORC is

passive, in the sense that no optimal thermodynamic parameter is actively set, but the pump working in safe operation is ensured [108]. Quoilin et al. [22] presented three different control strategies based on a PI controller for an ORC system with a scroll expander used for waste heat recovery from an ICE. In all three approaches, the pump speed and expander speed (scroll expander) were used as control variables. The first approach set constant evaporation temperature and degree of superheating; the second approach used an optimized evaporation temperature from an offline steady-state optimization, which was a function of the condensation temperature, heat source temperature and mass flow rate of the working fluid; the third approach set the pump speed according to the offline optimization as a function of the condensation temperature, heat source temperature and expander speed. The controller parameters were tuned manually. The second control strategy provides an overall better thermal performance of the ORC system than those of the first and third control approaches.

Ni et al. [33] investigated the dynamic performance of a solar ORC system with a scroll expander under cloudy conditions and proposed two conventional proportional–integral–derivative (PID) controllers for two control variables. The evaporation pressure and degree of superheating were controlled by manipulating the pump and expander speeds. The set points for both the evaporation pressure and the degree of superheating were kept constant. The results suggest that the cloud blockage of the sun for short periods (five minutes) does not affect the performance of the ORC system. For the specified simulation time (5000 s – 30 000 s), the system without the controller generated 84.95 kWh, while its counterpart with the PID control strategy generated 105.54 kWh, achieving an improvement of 24 %.

Luong et al. [109] developed the load-following control strategy for an ORC system that recovers the waste heat of a heavy-duty diesel powertrain. Three independent PI controllers controlled the evaporation pressure, condensing pressure, and the load demand. The mass flow rate of the sink fluid and two throttle valves were selected as manipulated variables. Li et al. [34] developed a dynamic model of a small-scale solar ORC system with a turbine including a thermal storage system. It was observed that for a specific solar period, there is a specific range of thermal storage system capacity that causes instability. It was concluded that the capacity of the thermal storage system should be carefully designed based on the local solar irradiation and dynamic response of the thermal storage system. A PI controller was used to ensure the stable operation of the system by maintaining a constant degree of superheating by manipulating the pump speed. Lin et al. [95] compared an ORC and an oil storage/ORC system recovering waste heat from an automotive internal-combustion engine. PID controllers were used for the ORC unit, which acted on the speed of the pump and the expander to control the evaporator pressure and degree of superheating. The integration of an intermediate oil storage could dampen the dynamic oscillations, but the costs per unit kW were higher than for a simple ORC unit.

Jolevski et al. [44] developed a control structure of an ORC system based on the non-square relative gain array and dynamic non-square relative gain array methods. A state-space model of the ORC unit was developed using a moving boundary approach for the heat exchangers and considering a turbine

with a control valve as the expander. The state-space model has been linearized, so that the coupling between the control variables (the turbine inlet pressure and temperature as well as the condensation pressure) and the manipulated variables (the mass flow rate of the coolant, the rotational speed of the pump and the opening of the turbine throttle valve) were analyzed. Approximated transfer functions, obtained from a Bode diagram (graph of the frequency response of a system), were used to get the optimal parameters of the control structure. The independent PI controllers were tuned to satisfy the robustness, phase margin of 45° , and high bandwidth. The proposed structure achieved satisfactory control performance for constant set points. Marchionni et al. [96] developed a dynamic model of a 40-kW ORC system with radial turbine and plate heat exchangers and compared four different control strategies. For all cases, the control variable is the turbine inlet temperature, which is kept at the nominal value, to achieve maximum power output, to avoid thermal degradation of the working fluid and to keep sufficient superheating at the turbine inlet. The control strategies differed in the choice of the manipulated variables: i) speed of the pump only; ii) speed of the turbine only; iii) speed of both the pump and the turbine; and iv) speed of the pump and recirculation from the pump to the condenser. PI controllers with anti-windup were chosen and calibrated based on the step response of the system. The turbine-based regulation strategies achieved better control performance, whereas the pump-based control strategies could keep the net power output closer to the design point for increase and decrease ramps of the heat source mass flow rate.

Imran et al. [97] developed a PID control strategy for waste heat recovery from long-haul trucks. The controllers were tested on a 45-minute run of a 450 hp 13 l long-haul truck engine. The control variable for every case was the degree of superheating at the turbine inlet, whose set point was set to 20 K. The controllers were tuned using the PID tuner application from MATLAB [110]. Two control strategies were investigated with the manipulated variables: i) the speed of the pump and a bypass valve for the exhaust gas flow entering the ORC evaporator; and ii) the speed of the pump and a throttling valve at the turbine inlet. The second control strategy could increase the net power output and outperform the first one.

Yang et al. [98] focused on a manager/controller structure of an ORC recovering waste heat from a vehicle, where the manager has an internal optimizer that defines the operational mode and optimizes the evaporating and condensing pressures, whereas the controller utilizes PIDs. The performance was simulated on the Highway Fuel Economy Test cycle. The degree of superheating could be kept within 5-15 K. In contrast to testing the controller in a simulation environment, Usman et al. [111] presented the implementation of a PI controller in an ORC unit with a scroll expander. The controller was compared with a PI with feed-forward and lead-lag compensator on an actual experimental rig.

A FCL strategy was followed, and the speed of the expander was the control variable. The speed of the pump was chosen as the manipulated variable. The PI controller was tuned following the Ziegler-Nichols rules. The solution with PI, feed-forward and lead-lag compensator could keep the expander speed within a relatively narrow range close to the set point, and the system recovered faster when a step load was imposed on the system; see Figure 11.

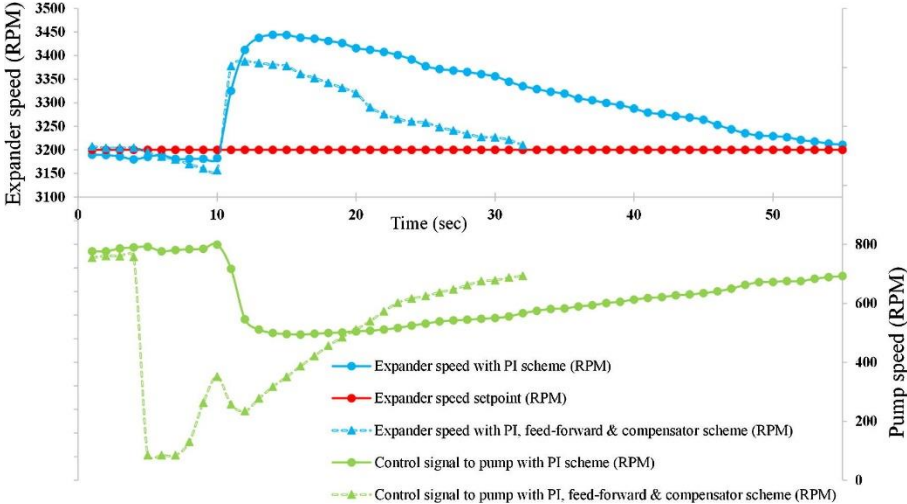


Figure 11: Tracking of the expander set point speed by different control approaches, Usman et al. [111].

Pili et al. [112] investigated the dynamic performance of an ORC unit recovering waste heat from a reheat billet furnace. The unit was controlled by three independent PI-controllers: the evaporator outlet temperature and pressure and the condensing pressure were controlled by, respectively, a bypass valve in the heat source line, the speed of the pump, and the speed of the cooling fans at the condenser. The set points were set by an offline steady-state, part-load optimization.

The system was subjected to a negative and a positive ramp in the waste heat mass flow rate and temperature. The deviations from the set points increased as the ramp rates became larger. The effect of the environmental conditions on the controller parameters for the same application was analyzed in [113]. The control studies involving PID-based controllers for ORC systems are listed in Table 4.

Table 4: PID-based control studies for organic Rankine cycle technology.

Ref.	Control approach		Manipulated Variables	Control variables	Disturbance variables
	System	Controller			
[22]	FTE	PI	N_{exp}, N_{pu}	SH, T_{ev}	\dot{m}_{hs}
[33]	FTE	PID	N_{exp}, N_{pu}	SH, p_{ev}	DNI
[109]	FCL	PI	$\mu_{tv,1}, \mu_{tv,2}, \dot{m}_{air}$	p_{ev}, p_{con}, W_{net}	$\dot{m}_{hs}, T_{hs}, T_{ss}$
[34]	FTE	PI	N_{pu}	N_{exp}	DNI
[114]	FTE	PID	N_{exp}, N_{pu}	SH, p_{ev}	\dot{m}_{hs}, T_{hs}
[44]	FTE	PI	$N_{exp}, N_{pu}, \dot{m}_{air}$	$p_{exp}, p_{con}, T_{exp}$	\dot{m}_{hs}
[115]	FTE	PI	$N_{exp}, N_{pu}, \mu_{tv}$	TIT	\dot{m}_{hs}
[116]	FTE	PID	$N_{pu}, \mu_{tv,1}$	SH	\dot{m}_{hs}, T_{hs}
[117]	FTE	PID	$N_{pu}, \mu_{tv,1}$	SH, p_{ev}	\dot{m}_{hs}, T_{hs}
[112]	FTE	PI	$\mu_{tv,1}, N_{pu}, N_{fans}$	$T_{exp}, p_{exp}, p_{con}$	\dot{m}_{hs}, T_{hs}
[111]	FCL	PI+FF+LLC	N_{pu}	W_{net}	W_{net}
[88]	FTE	PI+FF	\dot{m}_{wf}	T_{SH}	$\dot{m}_{hs}, T_{hs}, h_{wf}$

3.2 Optimal control

The optimal controller is based on a model of the ORC plant (differential equations) used to describe the path of the control variables that minimize the cost function or performance indexes. The common objective functions for the optimal control of ORC systems are thermal efficiency, net power output, control effort, closed-loop tracking error or a quadratic function as for the LQ control.

Peralez et al. [118] designed a controller maximizing the recovered energy of an ORC system that recovers waste heat on board a diesel-electric train:

$$J = \int_0^{t_f} [\dot{W}_{exp}(t) - \dot{W}_{pu}(t) - \dot{W}_{Aux}(t)] dt \quad (48)$$

The control law maximized the net power output acting on the mass flow rate of the engine exhaust gas via a bypass valve and on the mass flow rate of the condensing air, while keeping the wall temperature and pressure inside the evaporator within allowable limits. The optimal control problem was based on a simplified model of the system solved using dynamic programming and further improved by adaptive grids for discretization. The ORC evaporator and condenser were modeled as single-state systems.

The results suggest that a reasonable accuracy of the controller can be achieved with lower computational effort compared to the optimal control algorithm without adaptive grid. The trajectories of the optimal control provide detailed insight into the dynamic behavior of the system. In an extended version of the work [119], the authors address the issue of real-time operation and reformulate the problem so that dynamic programming is used as a supervisory control on the system, avoiding observability issues.

Zhang et al. [55] proposed a multi-objective estimation of the distribution algorithm to control the working fluid temperature at the evaporator outlet by manipulating the pump speed. The variation of the temperature difference between the set point temperature and the working fluid temperature at the evaporator outlet was minimized by tuning the controller to minimize simultaneously the squared mean value of the tracking error and the entropy of the superheated vapor temperature. The results indicate that the proposed approach can stabilize the superheated vapor temperature around the target value with small oscillations. The authors [120] approached the control problem of keeping the degree of superheating at the turbine inlet of an ORC system close to the set point and rejecting the disturbances in mass flow rate and temperature of the heat source, by using a single objective optimization. The optimal controller was obtained by minimizing an improved entropy criterion that combines the entropy of the tracking error, the mean value of the squared tracking error and the control effort. In addition, constraints on the rotational speed of the pump were considered. The proposed control algorithm obtained smaller overshoot and shorter settling time compared with a PID controller tuned in MATLAB. The comparison is shown in Figure 12.

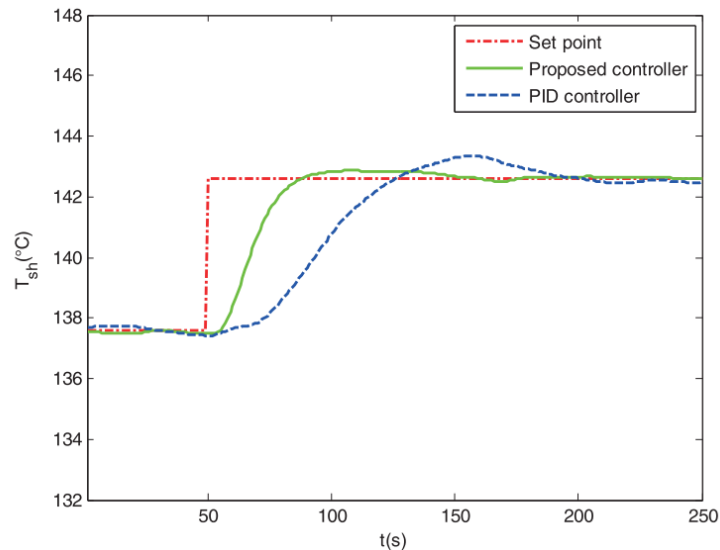


Figure 12: Response of superheated vapor temperature for the proposed controller and PID controller, Zhang et al. [120].

The approach was then further extended in [121] using a quantized information potential to characterize the quadratic entropy of the entropy error and a particle swarm optimization to achieve the optimal control law. The simulation confirmed the effectiveness of the method.

Zhang et al. [122] investigated the optimization of the set points of a controller of an ORC system to improve the energy conversion efficiency under varying operating conditions. The preliminary optimal set points of the ORC system were obtained by performing a performance analysis and optimization of the ORC system. Finally, the optimum evaporation pressure and working fluid temperature at the evaporator outlet were determined by combining the genetic algorithm with the least squares support vector machine (a machine learning and supervised learning model with associated learning algorithms that analyze data used for classification and regression analysis) [123]. Following the variation of the heat source, the optimal controller produces a signal to operate the expander at the optimum speed for maximum energy conversion efficiency.

Wu et al. [124] presented an offline optimal control design approach based on a mechanistic non-linear model of the ORC system. The objective of the optimum controller is to maximize the nominal net power output and to ensure safe operation of the ORC system during the presence of disturbances. The evaporation pressure, condensation pressure and degree of superheating were controlled by manipulating the pump speed, expander speed, and mass flow rate of the cooling air.

Ren et al. [125] proposed a single-neuron-based controller to control the evaporator outlet temperature of an ORC system. The survival information potential criterion was used to optimize the controller parameters, minimizing the randomness and magnitude of the closed-loop tracking error. The proposed neuro-controlled (NC) algorithm does not depend on the model of the controlled ORC process. In essence, this control algorithm is a data-driven control algorithm that can be implemented easily and can reject stochastic disturbances.

An important class of optimal controllers include the linear quadratic controllers. Luong et al. [126] employed two-input, two-output and three-input, two-output multi-variable quadratic integral controllers for an ORC system. The evaporation pressure and condensation pressure were used as control variables, while the flow rate of the condensing fluid and the position of the throttle valves placed before the evaporator and expander were used as manipulated variables.

The controller was designed through linearization in MATLAB. Larger weights on the quadratic cost function were chosen for the pressures and very low weights for the control inputs, related to their range of variability. The results suggest that the linear quadratic controller with three-input, two-output optimally determines the input-output relationship for pressure regulation; see Figure 13. The problem of state estimation was not addressed.

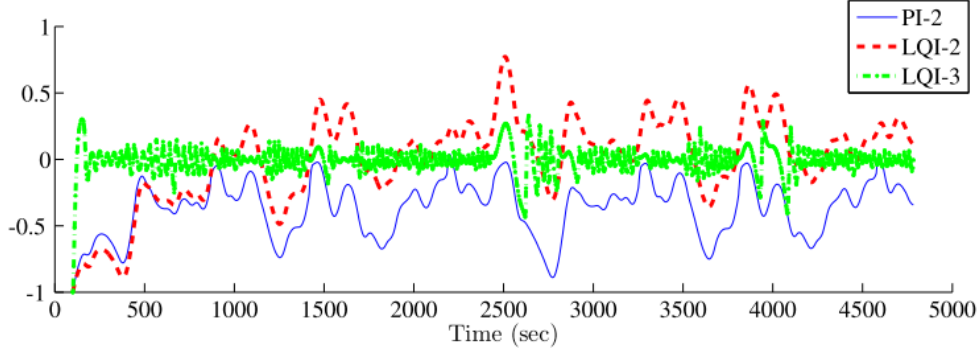


Figure 13: Controller regulation error of a non-linear controller based on 2- and 3-actuator configurations for an ORC system, Luong et al. [126].

Zhang et al. [64] presented a multi-variable control scheme of an ORC system used for waste heat recovery by incorporating a linear quadratic regulator with a PI controller in a simulation environment. The solution is equivalent to a linear quadratic integral controller with feed-forward, which was developed through linearization around the nominal point.

The problem of state estimation was not addressed. The manipulated variables were the opening of the throttling valve at the turbine inlet, the speed of the pump, and the velocity of the heat source and cold sink media, which with a multi-variable approach controlled the power output, the throttle pressure, and the outlet temperature of the working fluid leaving the evaporator and the condenser. The simulation provided good response against load tracking and disturbance rejection. The studies in the area of optimum control of the ORC systems are listed in Table 5. A comparison of the main advantages and disadvantages of each optimal control solution is illustrated in Table 6.

Table 5: Studies regarding optimum control strategies for organic Rankine cycle technology.

Ref.	Control approach		Manipulated Variables	Control variables	Disturbance variables
	System	Controller			
[118]	FTE	DP	$N_{pu}, \mu_{hs,1}$	p_{ev}, SH	\dot{m}_{hs}, T_{hs}
[119]	FTE	DP	N_{pu}, \dot{m}_{ss}	$p_{i,exp}, SH$	\dot{m}_{hs}, V_{hs}
[120]	FTE	NGS	N_{pu}	T_{SH}	\dot{m}_{hs}, T_{hs}
[55]	FTE	NGS	N_{pu}	$T_{o,ev}$	\dot{m}_{hs}, V_{hs}
[122]	FTE	OC	N_{pu}, N_{exp}	p_{ev}, SH	\dot{m}_{hs}, T_{hs}
[124]	FTE	OC	$N_{pu}, N_{exp}, \dot{m}_{ss}$	SH, p_{ev}, p_{con}	\dot{m}_{hs}, T_{hs}
[121]	FTE	NGS	ω_{pu}	SH	\dot{m}_{hs}, T_{hs}
[125]	FTE	NGS	N_{pu}	$T_{o,ev}$	\dot{m}_{hs}, T_{hs}
[126]	FCL	LQI	μ_{tv}, \dot{m}_{air}	p_{ev}, p_{con}	$\dot{m}_{hs}, T_{hs}, N_{pu}$
[64]	FCL	LQI	$V_{hs}, V_{ss}, N_{pu}, \mu_{tv}$	$p_{tv}, SH, W_{net}, T_{o,co}$	μ_{tv}, V_{hs}

Table 6: Advantages and disadvantages of optimal control strategies for organic Rankine cycle technology.

Controller	Advantages	Disadvantages
Dynamic Programming	<ul style="list-style-type: none"> • Applicable to both linear and non-linear systems • Real-time optimization of plant trajectory 	<ul style="list-style-type: none"> • High computational effort • Multi-variable approach, highly computationally expensive
Non-Gaussian stochastic control (minimum entropy criterion)	<ul style="list-style-type: none"> • Minimizes uncertainties in tracking error • Real-time optimization of control inputs • Multi-variable control possible 	<ul style="list-style-type: none"> • Real-time multi-objective optimization required
Data-driven set point optimization	<ul style="list-style-type: none"> • Allows for real-time optimization of plant trajectory • Adaptive algorithm can account for system aging and small variations 	<ul style="list-style-type: none"> • Training of estimating function, computationally expensive • Large data-set required for good accuracy • System modifications require new training
Linear quadratic control	<ul style="list-style-type: none"> • Simple, fast and robust algorithm • Can handle high order systems and multi-variable control 	<ul style="list-style-type: none"> • Requires system linearization • Weight matrices need to be chosen properly

3.3 Model predictive control

Model predictive control (MPC) is an efficient control approach for control of multi-variable systems while satisfying a set of constraints. In MPC, the difference between the predicted output and the desired reference is minimized online over a future horizon, subjected to constraints on the manipulated inputs, the system outputs and the states. A block diagram of a MPC controller is shown in Figure 14.

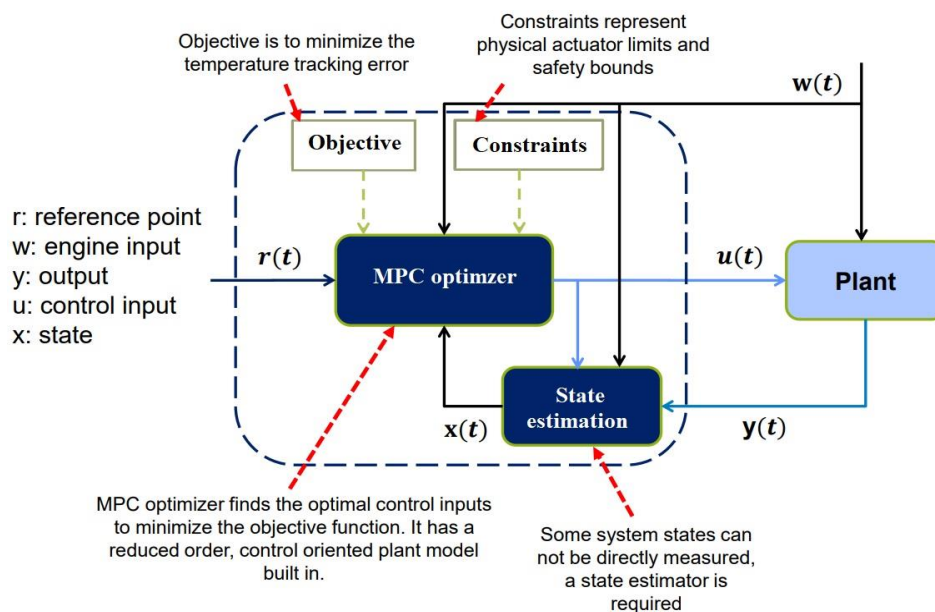


Figure 14: Basic structure of the model predictive controller, Liu et al. [39].

Liu et al. [39] implemented a model predictive controller on a small-scale ORC system, recovering the waste heat from a heavy-duty diesel engine exhaust tailpipe and exhaust gas recirculation (EGR) system. Two variants of a MPC (linear and non-linear) were implemented on a real-time embedded platform, and the performance of the controllers was compared with that of a traditional PID controller. The state estimation was carried out using a MB model of the evaporator. The pump speed was controlled to keep the expander inlet temperature at the set point. The results suggest that the MPC outperforms the PID controller and is able to keep the control variable within ± 10 °C under highly transient heat source conditions. Furthermore, the results indicate that the linear model predictive controller (LMPC) has better control stability for the control variable and outperforms the PID controller in terms of response time, overshoot, oscillations, and settling time; see Figure 15. Hernandez et al. [127] reported that a non-linear model predictive controller (NMPC) strategy leads to a smoother, safer and more efficient operation, resulting in a similar or better tracking performance at a lower control effort.

Hernandez et al. [128] presented an MPC strategy to increase the efficiency of an ORC system. The degree of superheating and evaporation temperature of the working fluid were controlled by manipulating the rotational speed of the working fluid pump and the single-screw expander. The results indicate that the Extended Prediction Self-Adaptive MPC algorithm provides higher efficiency of the ORC system than a decentralized PI controller. However, the variations of the heat source temperature and mass flow rate were less than ± 10 %.

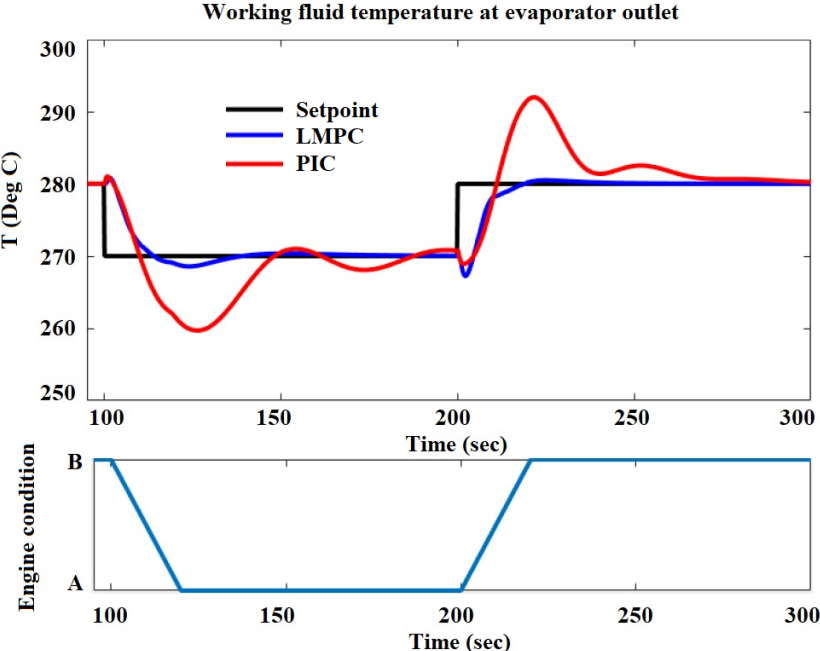


Figure 15: Temperature responses of LMPC and PID controllers for a step change in set point temperature and engine operating conditions, adapted from Liu et al. [39].

Subsequently, the authors extended the MPC strategy by optimizing the evaporation temperature under the constraints of the pump rotational speed and degree of superheating [129]. By taking a switching PI

as reference (100 %) of the net electrical energy produced, it was concluded that the basic MPC produces 15 % more energy, as it requires less control effort while keeping the unit in safe operation. The higher net power output is obtained by accurately optimizing the evaporation temperature, while keeping the degree of superheating within safe limits. However, the controller was evaluated for only ± 10 % variation of the heat source temperature and the mass flow rate.

Zhang et al. [130] presented a multiple MPC approach to deal with the non-linearity and varying operating conditions of ORC systems utilizing a transient heat source. The rotational speed of the pump and the shaft torque of the expander were manipulated simultaneously to provide the optimal evaporating pressure and superheating temperature. The operating range of the ORC system was divided into sub-operating regions, and the system response was represented by a CARIMA model. The predicted outputs of all sub-models and their corresponding weights were used to obtain the control signal. The simulation results suggest that the multiple MPC approach can effectively deal with non-linearity, constraints on the control variables, manipulated variables and varying operating points.

Pierobon et al. [131] implemented a linear MPC for offshore power stations with waste heat recovery using an ORC system. The MPC was coupled with a steady-state performance optimizer developed in SIMULINK/MATLAB [110]. The pump speed was varied to control the degree of superheating at turbine inlet. Transfer functions were achieved to reproduce the system dynamics. The system was able to cope with large disturbances effectively. Moreover, fuel savings and spared CO₂ emissions in the range of 2–3 % were obtained by introducing the steady-state performance optimizer.

Rahmani et al. [132] presented a constrained MPC strategy for an off-grid 4 kWe solar ORC system. The identification framework was used to identify non-linear maps for each variable of interest from the experimental real-time data. The net power output, degree of superheating, temperature of the working fluid at the inlet of the turbine and the pressure at the outlet of the turbine were used as control variables. The corresponding manipulated variables were the rotational frequency of the motor pump, the volume flow rate of the heat source, and the rotational speeds of the fan and the circulation pump. The ORC was able to provide the required electrical power under variations of hot source and cold sink inlet temperature with low settling time and good disturbance rejection.

Grelet et al. [133] employed an explicit multi-model MPC to control the degree of superheating at the inlet of the expander in an ORC-based waste heat recovery system mounted on a heavy-duty truck engine. The working fluid mass flow rate was chosen as the manipulated variable. The relationship between the manipulated variable and control variable defined in the non-linear single-input, single-output model was identified by a series of first-order plus time-delay models. The multi-model MPC controller based on the first-order plus time-delay model provides fast control, and it does not require online optimization and dynamic model resolution.

Feru et al. [56] presented a switching linear MPC strategy to reject disturbances caused by the diesel engine waste heat of the Euro-VI heavy-duty truck in real on-road driving conditions. The ORC system was based on a parallel evaporator configuration and two recirculation valves at the pump outlet that control the vapor quality at the outlet of each evaporator. The dynamic model resolution was improved by combining the finite difference modeling approach with a moving boundary model. The operating range of the ORC system was divided in three regions, and an MPC controller was assigned for each region. It was concluded that the switching linear MPC could achieve better control performance than PI controllers, and provided the vapor quality at the outlet of each evaporator within reasonable accuracy. A limitation of the proposed MPC strategy is the need of vapor fraction measurement equipment or an estimator for this quantity.

Petr et al. [134] optimized the net power output using a non-linear model predictive control approach of an ORC system which recovers waste heat from an internal-combustion engine of a vehicle. The target function for the MPC optimization problem was the ORC net power output. The manipulated variables were the speed of the pump and of the volumetric expander. The dynamic model was developed in the object-oriented programming language Modelica [135] using their model libraries TIL and TILMedia. The model was exported to MoBA Lab (simulation tool developed by TLK thermo) using a Functional Mockup Interface. The results indicate that the non-linear model predictive controller can improve the fuel economy by 8.1 % for a virtual drive test between Hanover and Munich in Germany. The MPC controller provides 7 % higher average net power output in part-load operation of the ICE than the conventional PI controller; see Figure 16.

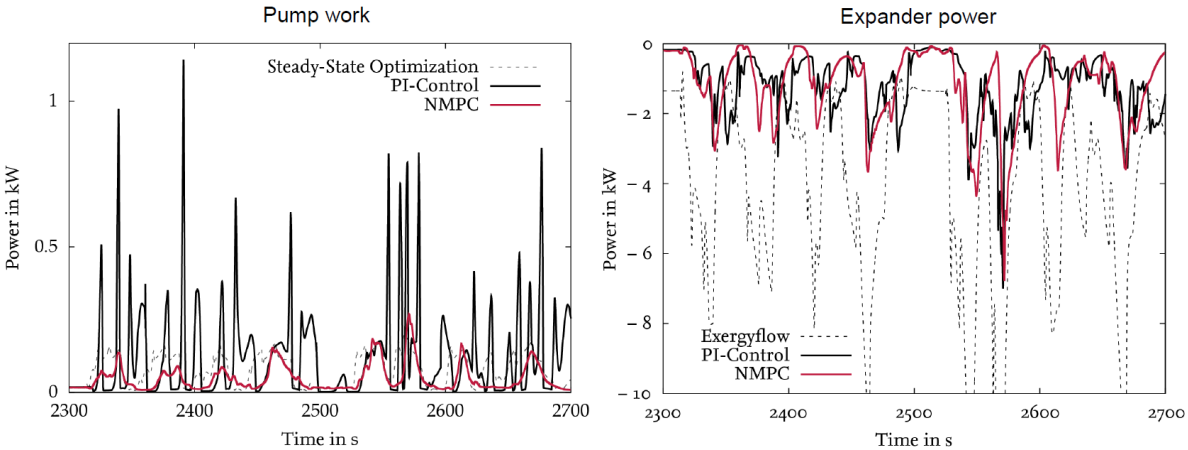


Figure 16: Pump work (left) and expander power output (right) of the ORC for both PI-control and non-linear model predictive controller, Petr et al. [134].

Hernandez et al. [136] developed and experimentally validated an adaptive MPC control law to maximize the power generation of a small-scale, ORC-based waste heat recovery system. The system dynamics were investigated by manipulating the variable pump speed to control the degree of superheating, and the corresponding changes in evaporation temperature and electrical power were analyzed at a specific value of the disturbances (mass flow rate and inlet temperature of the heat source).

The dynamic response of the system indicates that the evaporation temperature has a linear response, while the degree of superheating has a non-linear response with respect to changes in pump speed. Empirical correlations were developed based on a performance map of the system. Using an optimizer the optimal evaporation temperature was identified, while the degree of superheating was controlled by manipulating the pump rotational speed. Moreover, the MPC controller was successfully implemented on a lab-scale prototype. The experimental results indicate that the adaptive MPC produces about 17 % more electrical power compared to a gain-scheduled switching PID-based controller during 1800seconds of operation of the engine.

Luong et al. [58] developed a multi-variable MPC to estimate the states of the evaporator and condenser of an ORC system. The performance of the MPC was compared to proportional integral and linear quadratic integral (LQI) controllers. The system states (evaporator and condenser) were estimated by using extended Kalman filters. The results suggest that the MPC outperforms the PI and the LQI in terms of pressure regulation errors, since it can incorporate constraints on the control law.

Wu et al. [137] proposed an economic MPC scheme, where the controller set point is determined by the maximization of the net power output of the ORC unit. A MB model of the evaporator is reduced to a fourth-order model to reduce the computational effort. Both the expander and the pump speed are varied to reach the objective goal. Both the FTE and FCL modes are tested. The controller could optimize the power output with good performance.

Koppauer et al. [138] focused on an MPC strategy using a prediction model based on a gain-scheduling of a local, partially linearized system model. The state estimation is carried out with an EKF, where also the heat flow rates on the working fluid and heat source side were estimated to account for plant mismatches. The reference was provided by offline, steady-state optimization. The goal was to track the optimal trajectory. The controller showed sufficient tracking performance.

Rathod et al. [139] developed a non-linear MPC for an ORC recovering waste heat from a 13 l Diesel engine. The MPC was provided with an EKF for state estimation. The adaptability of the control strategy was proven by testing the controller under aging of the evaporator. The performance of the MPC was tested experimentally during a transient driving cycle, with the mean tracking error at 2.9 °C.

The previous studies utilizing the model predictive controller for the ORC system and the advantage and disadvantages of the main options are listed in Tables 7 and 8, respectively.

Table 7: Previous studies using the model predictive controller for organic Rankine cycle technology.

9.5	Control Approach		Process variables	Control variables	Disturbance variables
	system	controller			
[140]	FCL	GPC	$\mu_{tv,1}, v_{hs}, v_{ss}, N_{pu}$	$W_{net}, T_{SH}, p_{tv}, T_{co}$	W_{net}, V_{hs}
[39]	FTE	MPC	$\mu_{tv,1}, \omega_{pu}, \mu_{tv,2}, \dot{m}_{ss}$	$p_{ev}, T_{SH}, \Delta T, T_{co}$	\dot{m}_{hs}, T_{hs}
[128]	FTE	MPC	N_{pu}, N_{exp}	T_{SH}, SH	\dot{m}_{hs}, T_{hs}
[129]	FTE	MPC	N_{pu}	T_{SH}	\dot{m}_{hs}, T_{hs}
[130]	FTE	MPC	N_{pu}, τ_{exp}	p_{ev}, T_{SH}	τ_{exp}, N_{pu}
[57]	FTE	GPC	$N_{pu}, N_{exp}, \dot{m}_{ss}$	p_{ev}, SH, T_{co}	\dot{m}_{hs}, T_{hs}
[131]	FTE	MPC	μ_{tv}, N_{exp}	NT_f, SH	W_{net}
[132]	FCL	MPC	$N_{pu}, V_{hs}, N_{pu,ss}$	p_{ev}, W_{net}, T_{SH}	T_{hs}, T_{amb}
[133]	FTE	MPC	\dot{m}_{wf}	ΔT	\dot{m}_{hs}, T_{hs}
[56]	FTE	MPC	$\mu_{tv,1}, \mu_{tv,2}$	X_{hs1}, X_{hs2}	$N_{eng}, \dot{Q}_{hs1}, \dot{Q}_{hs2}$
[134]	FTE	MPC	N_{pu}, N_{exp}	W_{net}	\dot{m}_{hs}, T_{hs}
[136]	FTE	MPC	N_{pu}	p_{ev}, h_{SH}	\dot{m}_{hs}, T_{hs}
[137]	FCL	EMPC	\dot{m}_{wf}, N_{exp}	$p_{ev}, SH, T_{i,exp}$	\dot{m}_{hs}, T_{hs}
[58]	FTE	MPC+EKF	$\mu_{tv,1}, \mu_{tv,2}, \dot{m}_{air}$	p_{ev}, p_{con}	\dot{m}_{hs}, T_{hs}
[138]	FTE	MPC+EKF	$\dot{m}_{wf}, \mu_{hs,1}$	W_{net}	$\dot{m}_{hs}, T_{hs}, T_{amb}$
[139]	FTE	MPC+EKF	\dot{m}_{wf}	SH	\dot{m}_{hs}, T_{hs}

Table 8: Advantages and disadvantages of model predictive controllers for organic Rankine cycle technology.

Controller	Model	Advantages	Disadvantages
Linear model predictive controller with	Identification method	<ul style="list-style-type: none"> • Easy method • Does not necessarily require system model • Real-time optimization, has relatively low computational effort 	<ul style="list-style-type: none"> • Based on linear approximation • Might not be effective over a broad operational range • System modifications require new identification
	Model-based with linearization	<ul style="list-style-type: none"> • Can be easily developed for multi-models by linearizing on different operating point • Real-time optimization, has relatively low computational effort 	<ul style="list-style-type: none"> • Requires a system model • Based on linear approximation
Nonlinear model predictive controller	Identification method	<ul style="list-style-type: none"> • Identification is relatively simple • Does not necessarily require system model 	<ul style="list-style-type: none"> • System modifications require new identification • Nonlinear optimization problem increases computational burden
	Model-based	<ul style="list-style-type: none"> • Potentially, it can achieve the best control performance 	<ul style="list-style-type: none"> • Nonlinear optimization problem increases computational burden

3.4 Compound control approach

In the area of ORC control, it is common to use a compound control approach, consisting of two or more control techniques. Shi et al. [46] developed a compound control strategy, combining cascade control with two active disturbance rejection controllers, for an ORC-based engine waste heat recovery system. The exhaust gas flowing out of the evaporator was partially mixed and recirculated with the engine exhaust gas. The only control variable was the pressure of the evaporator, which was controlled by manipulating the mass flow rate of the engine exhaust gas using the exhaust gas recirculation (EGR) valve. The controller involved an extended observer based on a reformulation of a MB evaporator model. The results indicate that the control error of the evaporating pressure is lower than 0.1 %, and the fluctuation of the degree of superheating is less than 1 K; see Figure 17.

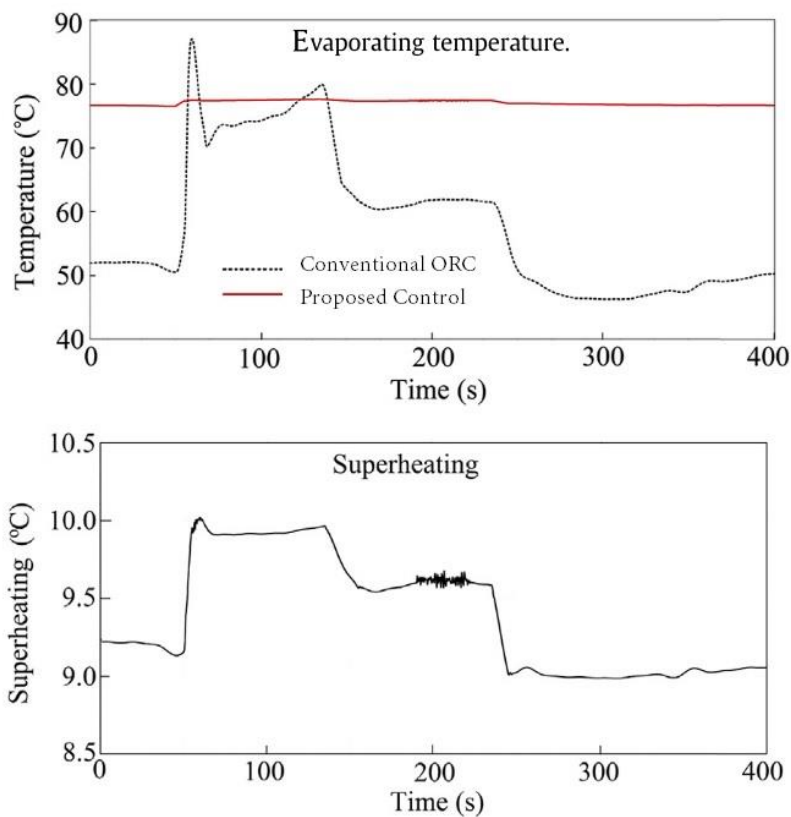


Figure 17: Degree of superheating and evaporation temperature control of an ORC system using a compound control strategy, Shi et al. [46].

Zhang et al. [141] proposed a combined control strategy for an ORC system, incorporating a linear active disturbance rejection (ADR) with a static decoupling compensator (DC). The disturbances were estimated through an extended linear state observer and then compensated by a linear feedback control strategy. The proposed control strategy does not require an accurate mathematical model of the system, therefore making it an appealing method for real applications. It requires instead extensive system identification to apply static decoupling. Simulation results indicate that the proposed control algorithm can provide good tracking performance and handle well disturbances for the waste heat recovery system, see Figure 18.

Yebi et al. [142] proposed a two-level controller structure for WHR with an ORC from a 13 l engine of a heavy-duty vehicle. A PID acted on the evaporator pressure reference controlling the bypass valve of the exhaust gas, whereas an MPC ensured optimal tracking of the mixed temperature at the outlet of two parallel evaporators. An UKF was used for state estimation. The innovative control structure could outperform a multiple-loop PID leading to 9 % more recovered thermal energy.

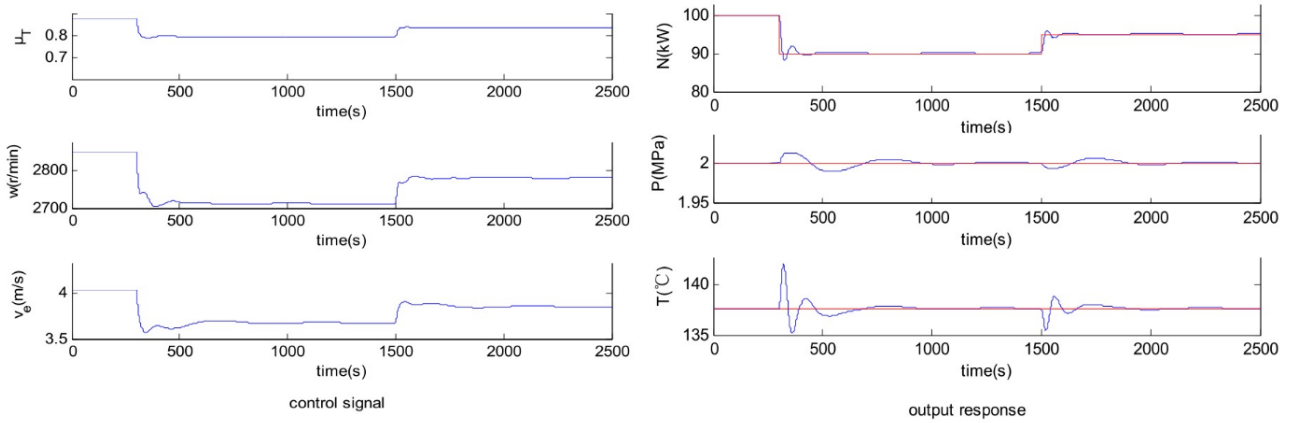


Figure 18: Response of controlled & manipulated variables of the combined control strategy, Zhang et al. [141].

Hernandez et al. [143] proposed a two-level, real-time optimization of a stationary sub-critical 11 kW ORC system by extremum-seeking control. Based on the results of the validated dynamic model, an empirical correlation for evaporating temperature was developed which maximizes the power generation for a range of operating conditions. The approach was extended to a perturbation-based extremum seeking algorithm to identify online the optimal evaporating temperature. The advantage of this algorithm is that it does not need a plant model. The low-level controller was then an EPSAC-MPC acting on the speed of the pump to track the optimal evaporating temperature (this one requires a model, developed here through parametric identification). A lower bound on the degree of superheating was also set as a constraint. The results indicate that the single PI controller acting on the degree of superheating rather than on the evaporating temperature can guarantee safe operation of the ORC system. In addition, it was concluded that the ESPAC-MPC strategy outperforms a PI-based controller in terms of energy generation. The previous studies using a compound control strategy are listed in Table 9, showing the manipulated variable and control variables. The advantages and disadvantages of the main concepts are illustrated in Table 10.

Table 9: List of studies based on compound control strategies for organic Rankine cycle technology.

Ref.	Control approach		Process variables	Control variables	Disturbance variables
	System	Controller			
[46]	FTE	ADRC+ESO	\dot{m}_{hs}	p_{ev}	\dot{m}_{hs}, T_{hs}
[141]	FCL	ADRC+ESO	$\mu_{tv,1}, N_{pu}, V_{hs}$	$T_{o,ev}, p_{tv}, W_{net}$	W_{net}
[142]	FTE	MPC+UKF + PID	$\dot{m}_{wf}, \mu_{hs,1}$	$T_{o,ev}, p_{ev}$	\dot{m}_{hs}, T_{hs}
[143]	FTE	ES+MPC	N_{pu}	$T_{o,ev}$	T_{hs}

Table 10: Advantages and disadvantages of compound control strategies for organic Rankine cycle technology.

Controller	Advantages	Disadvantages
Active disturbance rejection control with extended state observer	<ul style="list-style-type: none"> • Simple model development • Model uncertainties are compensated in real-time 	<ul style="list-style-type: none"> • Observer has to be fast compared to process dynamics • Observer tuning can be limited by sample time and noise on measurement
Nonlinear model predictive controller and PID	<ul style="list-style-type: none"> • Allows for multivariable control, especially for different time-scale controlled variables • Accounts for constraints through NMPC • Reduces computational burden for NMPC 	<ul style="list-style-type: none"> • Real-time constrained multi-objective optimization required
Extremum-seeking algorithm and model predictive control	<ul style="list-style-type: none"> • Real-time set point optimization • ES does not need a system model • Accounts for constraints through MPC 	<ul style="list-style-type: none"> • Multi-variable set point optimization becomes complex • Stability can be difficult to ensure

3.5 Additional advanced controllers

In order to tackle stochastic disturbances from the heat source and measurement noises, different types of controllers have been implemented for ORC systems, namely, minimum variance controllers, robust controllers, and neural controllers.

Hou et al. [59] employed an online, self-tuning, generalized minimum variance (GMV) controller for a 100 kW ORC-based waste heat recovery system. Online model identification was performed from the system input and output data. A controlled, autoregressive moving average model was used. The parameters were obtained using a recursive least squares (RLS) algorithm with a forgetting factor. The net power output, throttle pressure, degree of superheating, and the working fluid temperature at the condenser outlet were controlled by manipulating the throttle valve position (placed before the expander), pump rotational speed, mass flow rate of the exhaust gas, and velocity of the sink source (air). The result suggest that the GMV controller can effectively handle disturbances and ensure safe operation. Zhang et al. [144] developed a multi-variable robust controller for an ORC system. The evaporation pressure and degree of superheating were controlled by manipulating the pump and expander rotational speeds. The simulation results indicate that the proposed control strategy can obtain satisfactory performance in set point tracking and disturbance rejection operation. Such simply structured and easy-to-realized controller does not require a precise mathematical model to predict the dynamics of the system.

Wang et al. [145] designed and implemented a neuro-PID controller to control the outlet temperature of the evaporator in an ORC system used for waste heat recovery. The control variable was the velocity of the heat source (exhaust gas). The parameters of the PID controller were regulated using a back propagation neural network. However, the controller was developed only for the evaporator, and the rest of the components of the ORC system were not considered. Compared with a traditional PID control strategy, the proposed method could achieve better prediction for dynamic response and has strong robustness against parameter variations and external disturbances.

Torregrosa et al. [146] presented a compound control approach based on a PID controller with adaptive gains for an ORC-based engine waste heat recovery system. The temperature at the evaporator outlet and pressure were controlled by manipulating the rotational speeds of the pump and expander. The gains were adapted after experimental tests, based on offline maps as a function of the thermal power from the heat source and the error from the evaporator outlet temperature.

Padula et al. [147] developed a PI-based adaptive control system to control a geothermal ORC power plant. The purpose of the control system was to minimize the deviations from the design conditions when the plant is disconnected from the grid and put into island-mode operation. In this specific case, the dynamics and control mainly relate to the turbine and turbine bypass valves. When the ORC power plant is switched from the normal operation mode (grid-connected) to the island operation (standalone), an electric brake regulated by a non-linear feed-forward controller dissipates the excess of power produced in order to avoid excessive turbine speed overshoot.

Peralez et al. [60] presented a strategy to control the degree of superheating at the turbine inlet of an ORC system by combining a PID feedback controller with an implicit dynamic feed-forward controller. The PID controller was tuned based on an extensive system identification campaign. The dynamic feed-forward term was computed from a non-linear reduced model of the high-pressure part of the ORC system. Although the performance of the control of the degree of superheating is improved using the compound strategy, an extensive investigation of system identification is necessary in order to obtain a reliable, concise and efficient (short computational time) model.

In a recent study by the same authors [31] a controller combining gain-scheduling PID, feed-forward and implicit Extended Kalman Filters (EKF) approaches were experimentally evaluated. The system effectively controls the degree of superheating and the pressure at the turbine inlet, acting on the speed of the pump and bypass valve of the heat source. However, it needs to be pointed out that the magnitudes of the disturbances considered in the work are relatively small in comparison to, for example, the variations in heat source conditions that an ORC unit utilizing the exhaust gas of a truck engine would experience [148].

A similar approach was used by Grelet et al. [88] to control the outlet temperature of an ORC recovering waste heat from a long-haul truck by manipulating the speed of the pump. The PID controllers were

tested on a multi-model FOPTD identification of the ORC unit. The dynamic feed-forward could significantly improve the tracking performance of the controller. The most commonly used advanced control approaches for ORC systems are listed in Table 11, and their advantages and disadvantages are compiled in Table 12.

Table 11: List of the most commonly used advanced control strategies for organic Rankine cycle technology.

Ref.	Control approach		Manipulated variables	Control variables	Disturbance variables
	System	Controller			
[59]	FCL	MVC	$V_{hs}, V_{ss}, N_{pu}, \mu_{tv}$	$p_{tv}, SH, W_{net}, T_{o,co}$	W_{net}
[144]	FTE	RC	N_{pu}, N_{exp}	T_{ev}, SH	V_{hs}, T_{hs}
[145]	FTE	BPNN+PID	V_{hs}	$T_{o,ev}$	$\dot{m}_{wf}, V_{hs}, h_{i,ev}$
[146]	FTE	GS-PID	N_{pu}, N_{exp}	$T_{o,ev}, SH$	\dot{m}_{hs}, T_{hs}
[147]	FCL	GS-PI +FF	μ_{bppv}	N_{exp}	W_{net}
[60]	FTE	GS-PI+FF	N_{pu}	SH	\dot{m}_{hs}, T_{hs}
[31]	FTE	GS-PID+FF +EKF	$N_{pu}, \mu_{hs,1}$	p_{ev}, SH	\dot{m}_{hs}, T_{hs}
[88]	FTE	PID+FF	\dot{m}_{wf}	T_{SH}	$\dot{m}_{hs}, T_{hs}, h_{wf}$

Table 12: Advantages and disadvantages of the most commonly used advanced control strategies for organic Rankine cycle technology.

Controller	Advantages	Disadvantages
Generalized minimum variance	<ul style="list-style-type: none"> • Simple control law • Can reject stochastic disturbances 	<ul style="list-style-type: none"> • Response might be aggressive • Does not consider input effort in control law
Robust control	<ul style="list-style-type: none"> • Simple control law • Robust against uncertainties 	<ul style="list-style-type: none"> • Based on system linear approximation • Strict mathematical conditions have to apply
Neuro-PID	<ul style="list-style-type: none"> • Does not require system model • Can provide online tuning of PID 	<ul style="list-style-type: none"> • Quality of training set affects controller performance • System modifications require new training
Gain-scheduled PI or PID	<ul style="list-style-type: none"> • Good handling of nonlinearities of the system 	<ul style="list-style-type: none"> • Scheduling variable has to be chosen carefully to guarantee stability and good performance
Feedforward	<ul style="list-style-type: none"> • Good disturbance rejection • Good set point tracking 	<ul style="list-style-type: none"> • Requires system to be non-minimum phase or approximation necessary • Feedback might be required to account for uncertainties

4. Tools for dynamic modeling and controller design

Several commercial and open-source numerical tools are available for steady-state and dynamic process simulation of thermal power plants including the ORC process. MATLAB/SIMULINK and MODELICA are the most commonly used for dynamic modeling and control of ORC systems. The former allows both for graphical and text-based programming, and has a large number of toolboxes developed for controller design, system identification and optimization. The MODELICA language is used by DYMOLA, JModelica.org and SimulationX, and it has been specifically developed for the solution of differential algebraic systems, which are common in the fields of thermal, chemical, electrical and mechanical engineering. Different free and commercial libraries in MODELICA language are available, with already built-in models. In contrast to Simulink, modeling in MODELICA is acausal; the equations are rearranged by the software according to the solution algorithm without the need of a priori in/out sequential form, which represents a big advantage for the modeling of nonlinear thermo-fluid systems as ORC systems. APROS, ASPEN Plus Dynamics, PPSD and TRNSYS are proprietary commercial software with built-in dynamical models of the main plant components. The user has however limited freedom in the extension of the available models. For example, the software might prevent the possibility to test or integrate unconventional heat exchanger geometries or turbomachinery, as well as novel heat transfer and pressure drop correlations. Other software are available, but hardly used in the field of organic Rankine cycle power systems. Commercial numerical tools for the dynamic process simulation of thermal power plants are listed in Table 13.

Table 13: List of commercial software for dynamic modeling and control of thermal power plants, from Alobaid et al. [70].

No.	Program	Developer	Website
1	APROS	Technical Research Center of Finland	http://www.apros.fi/en
2	ASPEN Plus Dynamics	Aspen Technology, Inc.	https://www.aspentech.com
3	DYMOLA	Dassault Systèmes	http://www.3ds.com
4	gPROMS Platform	Process Systems Enterprise Limited	http://www.psenderprise.com
5	JModelica.org	Modelon AB	http://www.jmodelica.org/
6	MATHEMATICA	Wolfram Research	https://www.wolfram.com/mathematica
7	SIMULINK	The MathWorks, Inc.	https://www.mathworks.com
8	PPSD	KED GmbH	http://www.ked.de/index.html?&L=1
9	ProTRAX Software	TRAX Energy Solutions	https://energy.traxintl.com
10	EASY5, etc.	MSC Software	http://www.mscsoftware.com
11	EcosimPro, PROOSIS.	Empresarios Agrupados A.I.E	http://www.ecosimpro.com
12	SimSci, DYNMIM	Schneider Electric Software	http://software.schneider-electric.com
13	SimulationX	ITI GmbH	https://www.simulationx.com
14	RELAP	Idaho National Laboratory	http://energy.gov
15	TRNSYS	University of Wisconsin	http://sel.me.wisc.edu/trnsys
16	UniSim Design	Honeywell	https://www.honeywellprocess.com
17	3-Key Master	Western Services Corporation	https://www.ws-corp.com

5. Concluding remarks

The dynamic response of the organic Rankine cycle system depends on the heat source, system size, operating conditions, type of equipment and working fluid to some extent. There are large variations in these parameters among organic Rankine cycle systems. It can be concluded that each organic Rankine cycle system will have unique dynamic response characteristics and control strategy, and hence, there are no established standard design rules or clear best practices in this field. Based on the review of the previous works concerning dynamic modeling of organic Rankine cycle systems, the following conclusions are drawn:

- The dynamics of the organic Rankine cycle system is mainly governed by the heat exchangers. The heat exchangers account for the majority of performance lag due to dynamic changes in operating conditions. There are three approaches for dynamic modeling of the evaporator and condenser of the organic Rankine cycle system, namely, moving boundary, finite volume and two-volume models. The moving boundary approach has lower computational time, but higher prediction error compared to those of the finite volume approach. However, the computational time of the finite volume method can be reduced by selecting an optimum level of discretization. The two-volume approach is applicable only for phase change in a shell. The addition of the heat transfer and pressure drop correlations results in a larger computational effort and higher accuracy. The time constants characterizing the expansion and compression processes are small compared to those of the evaporator and condenser. Thus, the expander and pump models are typically based on steady-state, lumped parameter models. If performance maps of these components are available, non-dimensional parameters can be used to predict their performances. The dynamic characteristics of control valves are typically modeled with relevant equations that correlate the valve opening, boundary conditions and the flow through the component. If the system dynamics are fast, the valve positioning servo-system plays an important role to determine the closed-loop dynamic behavior of the system and should therefore be included in the model. However, it is difficult to gain access to the information about the servo-positioner dynamics; hence, first-order or second-order linear systems can be used to consider these dynamics. If experimental data are available, an empirical correlation can be developed to calculate the mass flow rate for incompressible flow (or the equivalent) based on the relative valve opening.
- Measuring instruments may have a significant delayed response, especially temperature sensors. If the time-scale of a given measuring instrument is not negligible compared to the closed-loop response time, the response time of the measuring instrument should be included in the dynamic model.
- Dynamic models have been matched to experimental data with reasonable accuracy. In most of the cases, the relative deviation is different among the observed parameters. For instance, the turbine inlet temperature may have a different relative deviation than the condenser pressure of the same

system in dynamic operation. Previous work indicate that if the models are calibrated properly, dynamic models can predict the process variables within a 3% relative deviation from the experimental results.

The control of the organic Rankine cycle systems plays an important role in terms of the system performance and safe operation. In this paper, different control techniques and findings of previous research work in the area of control systems of organic Rankine cycle systems were reviewed and discussed. The prospects and constraints of the different control techniques and their limitations were analyzed and discussed. Some important points concerning the development of controllers for organic Rankine cycle systems can be summarized as follows:

- The complexity of the control system and corresponding control strategy depends on the operation (grid-connected or off-grid) of the organic Rankine cycle system.
- The model predictive controller, especially improved model predictive control (multiple model predictive control, switching model predictive control, non-linear model predictive control), provides excellent control performance as it can deal with non-linearity, process constraints, and a wide range of system disturbances efficiently.
- Although the control strategies proposed for organic Rankine cycle systems depend on the dynamic model of the system, a few authors presented control-oriented models, such as two-state models [119], simplified physical models [22,149], first-order plus dead-time model [150], and the transfer functions-based model [128].
- There exists an optimal rotational speed for an expander that corresponds to its maximum isentropic efficiency for specific operating conditions. It is necessary to investigate both the machine-side and grid-side controller for organic Rankine cycle power generation systems. For optimal operation of organic Rankine cycle systems, the use of a supervisory control strategy could be helpful to produce optimal set points for the control system.
- Since the dynamic response of the organic Rankine cycle system is complex in terms of non-linearity, coupling and time variation disturbances, the use of advanced control algorithms is helpful.
- Organic Rankine cycle systems are extremely diversified in terms of applications, operating conditions, size, and type of equipment; therefore, the optimal control strategy may be different for each system. In order to identify the optimal control strategy for a given system, a comparative analysis of the performance of different control strategies based on system performance, tracking error, overshoot, rise time, settling time, peak time, robustness to disturbances, handling constraints, computational effort, and practical implementation needs to be conducted.
- Almost all of the previous studies analyzed the performance of the controller under a range of variation of the input disturbances typically smaller than those occurring during operation of

organic Rankine cycle systems utilizing highly transient heat sources in practice. In order to adapt to fluctuations in the heat sources or connected load, the performance of the controller needs to be evaluated over a wide (or entire) operating range of the system, ensuring safe and optimal operation of the organic Rankine cycle system.

As far as recommendations for future research are concerned, first it needs to be stressed that in almost all of the previous works, the design and component sizing of the organic Rankine cycle system were based on the heat sink and heat source conditions without taking into account the dynamic response and control of the system. Such design and optimization approach may lead to an organic Rankine cycle system that is sensitive to highly transient heat sources and difficult to operate in a safe and efficient manner. Therefore, for future research and design practice of organic Rankine cycle systems utilizing highly fluctuating heat sources, we recommend to include the dynamic response and control aspects into the preliminary design of the system in an iterative manner. Such approach will discard the designs that feature unacceptable dynamic performance in an early phase of the design process and will support the selection of the best possible combination of on-design, off-design, and dynamic performances, while fulfilling at the same time all the constraints in terms of the operational parameters of the system.

Most of the experimental work discussed the experimental validation of dynamic models which involved matching of response time and steady-state error for a measured/known disturbance. There are limited works which compared the efficacy of different types of controllers. There is an urgent need to implement the proposed controller on a real ORC system and assess the performance of the controller under changing heat source or sink conditions. Besides, it is essential to test the different control strategies on the same test rig under the same disturbance for a fair comparison of the different control schemes.

The start-up and shut-down control methods had not been reported in open literature yet, except few patents. The start-up and shut-down control methods for transient heat source are critical and require additional safety measures. There is a need for implementation to investigate control narratives, which discuss start-up and shut down to ensure safe operation and avoid thermal shocks.

Acknowledgement

The research presented in this paper has received funding from the European Union's Horizon 2020 research and innovation programme with a Marie Skłodowska-Curie Fellowship under grant agreement number 751947 (project DYNCON-ORC), as well as the grant agreement number 754462 (EuroTechPostdoc, project ACT-ORC). The financial support is gratefully acknowledged.

Nomenclature

Abbreviations

AC	Adaptive control
ADRC	Active disturbance rejection controller
BPNN	Back propagation neural network
CC	Cascade control
CV _r	Control variable
CARMA	Controlled autoregressive moving average
DC	Decoupling compensator
DNI	Direct normal irradiance
DNRGA	Dynamic non-square relative gain array
DP	Dynamic programming
EGR	Exhaust gas recirculation
FF	Feed-forward controller
FCL	Following connected load
FTE	Following thermal energy
FV	Finite volume method
EKF	Extended Kalman filters
GS	Gain scheduling
GMV	Generalized minimum variance
ICE	Internal combustion engine
LLC	Lead-lag compensator
LMPC	Linear model predictive controller
LQ	Linear quadratic
LQI	Linear quadratic integral
LQR	Linear quadratic regulator
MAC	Model algorithmic control
MB	Moving boundary method
MPC	Model predictive controller
NC	Neuro control
NGS	Non-gaussian system control
NRGA	Non-square relative gain array
OC	Optimum control
ORC	Organic Rankine cycle
PR	Pressure ratio
PV _r	Process variable
PID	Proportional integral derivative
PI	Proportional integral
PMSG	Permanent magnet synchronous generator
RC	Robust control
RLS	Recursive least squares
SH	Superheat
TIT	Turbine inlet temperature
WHR	Waste heat recovery

Symbols

A	Area, m ²
c_p	Specific heat capacity, J/kg.K
D_{eq}	Effective flow path diameter
f	Frequency, Hz
J	Total recovered energy, J
h	Specific enthalpy, kJ/kg
L	Length, m
\dot{m}	Mass flow rate, kg/s
N	Speed, rpm
p	Pressure, Pa
\dot{Q}	Heat transfer rate, kJ/s
r	Non-dimensional pressure ratio
T	Temperature, °C
t	Time, seconds
U	Overall heat transfer coefficient, W/(m ² .K)
U	Internal energy, J
V	Volume, m ³
V_s	Swept volume, m ³
v	Velocity, m/s
x	Quality, -
Y	Level of saturated liquid in storage tank, -
W	Power, W

Subscripts and superscripts

Bpv	Turbine bypass valve
Co	Condenser
cv	Control valve
$Corr$	Correlation
$Const$	Constant
Ev	Evaporator, evaporation
eng	Engine
exp	Expander
f	Single-phase state (liquid)
g	Single-phase state (gas)
hs	Heat source
i	Cell index i
in	in
is	Isentropic
liq	Liquid state
n	Nominal condition
net	Net (with reference to net power output)
out	Out
pd	Pump displacement
pu	Pump
sw	Swept volume

<i>ss</i>	Sink source
<i>tv</i>	<i>Throttle valve</i>
<i>tp</i>	Two-phase
<i>vp</i>	Vapor state
<i>vol</i>	volumetric
<i>w</i>	wall
<i>wf</i>	Working fluid
<i>XA</i>	Cross-sectional area
<i>z</i>	<i>Spatial position</i>

Greek letters

η	Efficiency, %
α	Heat transfer coefficient, W/(m ² .K)
ρ	Density, kg/m ³
ϕ	Filling Factor, -
γ	Heat capacity ratio, -
Δ	Difference
η_{ϵ}	Heat exchanger efficiency multiplier, %
μ	Valve position, -
τ	Torque, N.m

References

- [1] Colonna P, Casati E, Trapp C, Mathijssen T, Larjola J, Turunen-Saaresti T, et al. Organic Rankine Cycle Power Systems: From the Concept to Current Technology, Applications, and an Outlook to the Future. *J Eng Gas Turbines Power* 2015;137:100801. doi:10.1115/1.4029884.
- [2] Forman C, Muritala IK, Pardemann R, Meyer B. Estimating the global waste heat potential. *Renew Sustain Energy Rev* 2016;57:1568–79. doi:10.1016/j.rser.2015.12.192.
- [3] Imran M, Park B-S, Kim H-J, Lee D-H, Usman M. Economic assessment of greenhouse gas reduction through low-grade waste heat recovery using organic Rankine cycle (ORC). *J Mech Sci Technol* 2015;29:835–43. doi:10.1007/s12206-015-0147-5.
- [4] Tchanche BF, Lambrinos G, Frangoudakis a., Papadakis G. Low-grade heat conversion into power using organic Rankine cycles – A review of various applications. *Renew Sustain Energy Rev* 2011;15:3963–79. doi:10.1016/j.rser.2011.07.024.
- [5] Sprouse C, Depcik C. Review of organic Rankine cycles for internal combustion engine exhaust waste heat recovery. *Appl Therm Eng* 2013;51:711–22. doi:10.1016/j.applthermaleng.2012.10.017.
- [6] Mondejar ME, Andreasen JG, Pierobon L, Larsen U, Thern M, Haglind F. A review of the use of organic Rankine cycle power systems for maritime applications. *Renew Sustain Energy Rev* 2018;91:126–51. doi:10.1016/j.rser.2018.03.074.
- [7] Campana F, Bianchi M, Branchini L, De Pascale A, Peretto A, Baresi M, et al. ORC waste heat recovery in European energy intensive industries: Energy and GHG savings. *Energy Convers Manag* 2013;76:244–52. doi:10.1016/j.enconman.2013.07.041.
- [8] Bianchi M, Branchini L, De Pascale A, Melino F, Peretto A, Archetti D, et al. Feasibility of ORC application in natural gas compressor stations. *Energy* 2019;173:1–15. doi:10.1016/j.energy.2019.01.127.
- [9] Hoang AT. Waste heat recovery from diesel engines based on Organic Rankine Cycle. *Appl Energy* 2018;231:138–66. doi:10.1016/j.apenergy.2018.09.022.
- [10] Shi L, Shu G, Tian H, Deng S. A review of modified Organic Rankine cycles (ORCs) for internal combustion engine waste heat recovery (ICE-WHR). *Renew Sustain Energy Rev* 2018;92:95–110. doi:10.1016/j.rser.2018.04.023.
- [11] Lion S, Michos CN, Vlaskos I, Rouaud C, Taccani R. A review of waste heat recovery and Organic Rankine Cycles (ORC) in on-off highway vehicle Heavy Duty Diesel Engine applications. *Renew Sustain Energy Rev* 2017;79:691–708. doi:10.1016/j.rser.2017.05.082.

- [12] Zhou F, Joshi SN, Rhoté-Vanay R, Dede EM. A review and future application of Rankine Cycle to passenger vehicles for waste heat recovery. *Renew Sustain Energy Rev* 2016;75:1008–21. doi:10.1016/j.rser.2016.11.080.
- [13] Zhai H, An Q, Shi L, Lemort V, Quoilin S. Categorization and analysis of heat sources for organic Rankine cycle systems. *Renew Sustain Energy Rev* 2016;64:790–805. doi:10.1016/j.rser.2016.06.076.
- [14] Lecompte S, Huisseune H, Van Den Broek M, Vanslambrouck B, De Paepe M. Review of organic Rankine cycle (ORC) architectures for waste heat recovery. *Renew Sustain Energy Rev* 2015;47. doi:10.1016/j.rser.2015.03.089.
- [15] Imran M, Haglind F, Asim M, Zeb Alvi J. Recent research trends in organic Rankine cycle technology: A bibliometric approach. *Renew Sustain Energy Rev* 2018;81:552–62. doi:10.1016/j.rser.2017.08.028.
- [16] Landelle A, Tauveron N, Haberschill P, Revellin R, Colasson S. Organic Rankine cycle design and performance comparison based on experimental database. *Appl Energy* 2017;204:1172–87. doi:10.1016/j.apenergy.2017.04.012.
- [17] Park BS, Usman M, Imran M, Pesyridis A. Review of Organic Rankine Cycle experimental data trends. *Energy Convers Manag* 2018;173:679–91. doi:10.1016/j.enconman.2018.07.097.
- [18] Muhammad U, Imran M, Lee DH, Park BS. Design and experimental investigation of a 1 kW organic Rankine cycle system using R245fa as working fluid for low-grade waste heat recovery from steam. *Energy Convers Manag* 2015;103:1089–100. doi:10.1016/j.enconman.2015.07.045.
- [19] Colonna P, van Putten H. Dynamic modeling of steam power cycles. Part I-Modeling paradigm and validation. *Appl Therm Eng* 2007;27:467–80. doi:10.1016/j.applthermaleng.2006.06.011.
- [20] van Putten H, Colonna P. Dynamic modeling of steam power cycles: Part II - Simulation of a small simple Rankine cycle system. *Appl Therm Eng* 2007;27:2566–82. doi:10.1016/j.applthermaleng.2007.01.035.
- [21] Wei D, Lu X, Lu Z, Gu J. Dynamic modeling and simulation of an Organic Rankine Cycle (ORC) system for waste heat recovery. *Appl Therm Eng* 2008;28:1216–24. doi:10.1016/j.applthermaleng.2007.07.019.
- [22] Quoilin S, Aumann R, Grill A, Schuster A, Lemort V, Spliethoff H. Dynamic modeling and optimal control strategy of waste heat recovery Organic Rankine Cycles. *Appl Energy* 2011;88:2183–90. doi:10.1016/j.apenergy.2011.01.015.
- [23] Casella F, Mathijssen T, Colonna P, Buijtenen J Van, van Buijtenen J. Dynamic Modeling of Organic

- Rankine Cycle Power Systems. *J Eng Gas Turbines Power* 2013;135:042310. doi:10.1115/1.4023120.
- [24] Casella F, Leva A. Modelica open library for power plant simulation: design and experimental validation. *Proc. 3rd Int. Model. Conf.*, 2003, p. 41–50.
- [25] Wronski J, Lemort V, Quoilin S, Bell I, Desideri A. ThermoCycle: A Modelica library for the simulation of thermodynamic systems. *Proc 10th Int Model Conf* 2014;96:683–92. doi:10.3384/ecp14096683.
- [26] Pierobon L, Casati E, Casella F, Haglind F, Colonna P. Design methodology for flexible energy conversion systems accounting for dynamic performance. *Energy* 2014;68:667–79. doi:10.1016/j.energy.2014.03.010.
- [27] Lakhani S, Raul A, Saha SK. Dynamic modelling of ORC-based solar thermal power plant integrated with multitube shell and tube latent heat thermal storage system. *Appl Therm Eng* 2017;123:458–70. doi:10.1016/j.applthermaleng.2017.05.115.
- [28] Huster WR, Vaupel Y, Mhamdi A, Mitsos A. Validated dynamic model of an organic Rankine cycle (ORC) for waste heat recovery in a diesel truck. *Energy* 2018;151:647–61. doi:10.1016/j.energy.2018.03.058.
- [29] Shu G, Wang X, Tian H, Liu P, Jing D, Li X. Scan of working fluids based on dynamic response characters for Organic Rankine Cycle using for engine waste heat recovery. *Energy* 2017;133:609–20. doi:10.1016/j.energy.2017.05.003.
- [30] Palagi L, Pesyridis A, Sciubba E, Tocci L. Machine Learning for the prediction of the dynamic behavior of a small scale ORC system. *Energy* 2019;166:72–82. doi:10.1016/j.energy.2018.10.059.
- [31] Peralez J, Nadri M, Dufour P, Tona P, Sciarretta A. Organic Rankine Cycle for Vehicles : Control Design and Experimental Results. *IEEE Trans Control Syst Technol* 2016;25:1–14.
- [32] Dickes R, Dumont O, Daccord R, Quoilin S, Lemort V. Modelling of organic Rankine cycle power systems in off-design conditions: An experimentally-validated comparative study. *Energy* 2017;123:710–27. doi:10.1016/j.energy.2017.01.130.
- [33] Ni J, Zhao L, Zhang Z, Zhang Y, Zhang J, Deng S, et al. Dynamic performance investigation of organic Rankine cycle driven by solar energy under cloudy condition. *Energy* 2018;147:122–41. doi:10.1016/j.energy.2018.01.032.
- [34] Li S, Ma H, Li W. Dynamic performance analysis of solar organic Rankine cycle with thermal energy storage. *Appl Therm Eng* 2018;129:155–64. doi:10.1016/j.applthermaleng.2017.10.021.
- [35] Xu B, Yebi A, Onori S, Filipi Z, Liu X, Shetty J, et al. Transient Power Optimization of an Organic

- Rankine Cycle Waste Heat Recovery System for Heavy-Duty Diesel Engine Applications. SAE Int J Altern Powertrains 2017;6:2017-01-0133. doi:10.4271/2017-01-0133.
- [36] Xu B, Liu X, Shutty J, Ansel P, Onori S, Filipi Z, et al. Physics-Based Modeling and Transient Validation of an Organic Rankine Cycle Waste Heat Recovery System for a Heavy-Duty Diesel Engine. SAE Tech Pap 2017;2016-01-01. doi:10.4271/2016-01-0199. Copyright.
- [37] Liu L, Pan Y, Zhu T, Gao N. Numerical predicting the dynamic behavior of heat exchangers for a small-scale Organic Rankine Cycle. Energy Procedia 2017;129:419–26. doi:10.1016/j.egypro.2017.09.127.
- [38] Samiuddin J, Badkoubeh-Hezaveh B, Sadeghassadi M, Pieper JK, Macnab CJB. Nonlinear adaptive control of a transcritical Organic Rankine Cycle. 2017 IEEE 26th Int Symp Ind Electron 2017:513–9. doi:10.1109/ISIE.2017.8001299.
- [39] Liu X, Yebi A, Ansel P, Shutty J, Xu B, Hoffman M, et al. Model Predictive Control of an Organic Rankine Cycle System. Energy Procedia 2017;129:184–91. doi:10.1016/j.egypro.2017.09.109.
- [40] Wang X, Shu G, Tian H, Liu P, Li X, Jing D. Engine working condition effects on the dynamic response of organic Rankine cycle as exhaust waste heat recovery system. Appl Therm Eng 2017;123:670–81. doi:10.1016/j.applthermaleng.2017.05.088.
- [41] Ni J, Wang Z, Zhao L, Zhang Y, Zhang Z, Ma M, et al. Dynamic simulation and analysis of Organic Rankine Cycle system for waste recovery from diesel engine. Energy Procedia 2017;142:1274–81. doi:10.1016/j.egypro.2017.12.485.
- [42] Galindo J, Dolz V, Royo-Pascual L, Brizard A. Dynamic Modeling of an Organic Rankine Cycle to recover Waste Heat for transportation vehicles. Energy Procedia 2017;129:192–9. doi:10.1016/j.egypro.2017.09.111.
- [43] Wang X, Shu G, Tian H, Liu P, Jing D, Li X. Dynamic analysis of the dual-loop Organic Rankine Cycle for waste heat recovery of a natural gas engine. Energy Convers Manag 2017;148:724–36. doi:10.1016/j.enconman.2017.06.014.
- [44] Jolevski D, Bego O, Sarajcev P. Control structure design and dynamics modelling of the organic Rankine cycle system. Energy 2017;121:193–204. doi:10.1016/j.energy.2017.01.007.
- [45] Grelet V, Reiche T, Lemort V, Nadri M, Dufour P. Transient performance evaluation of waste heat recovery rankine cycle based system for heavy duty trucks. Appl Energy 2016;165:878–92. doi:10.1016/j.apenergy.2015.11.004.
- [46] Shi R, He T, Peng J, Zhang Y, Zhuge W. System design and control for waste heat recovery of automotive engines based on Organic Rankine Cycle. Energy 2016;102:276–86. doi:10.1016/j.energy.2016.02.065.

- [47] Desideri A, Hernandez A, Gusev S, van den Broek M, Lemort V, Quoilin S. Steady-state and dynamic validation of a small-scale waste heat recovery system using the ThermoCycle Modelica library. *Energy* 2016;115:684–96. doi:10.1016/j.energy.2016.09.004.
- [48] Carolina S, Xu B, Carolina S, Carolina S, Hoffman M. Nonlinear model predictive control strategies for a parallel evaporator diesel engine waste heat recovery system. *ASME 2016 Dyn. Syst. Control Conf.*, Minnesota, USA: 2016, p. 1–9.
- [49] Proctor MJ, Yu W, Kirkpatrick RD, Young BR. Dynamic modelling and validation of a commercial scale geothermal organic rankine cycle power plant. *Geothermics* 2016;61:63–74. doi:10.1016/j.geothermics.2016.01.007.
- [50] Seitz D, Gehring O, Bunz C, Brunschier M, Sawodny O. Dynamic Model of a Multi-Evaporator Organic Rankine Cycle for Exhaust Heat Recovery in Automotive Applications. *IFAC-PapersOnLine* 2016;49:39–46. doi:10.1016/j.ifacol.2016.10.508.
- [51] Grelet V, Lemort V, Nadri M, Dufour P, Reiche T, Tilman S, et al. Waste Heat Recovery Rankine Cycle Based System Modeling for Heavy Duty Trucks Fuel Saving Assessment. *Proc 3rd Int Semin ORC Power Syst* 2015;1:1–10.
- [52] Esposito MC, Pompini N, Gambarotta A, Chandrasekaran V, Zhou J, Canova M. Nonlinear model predictive control of an Organic Rankine Cycle for exhaust waste heat recovery in automotive engines. *IFAC-PapersOnLine* 2015;28:411–8. doi:10.1016/j.ifacol.2015.10.059.
- [53] Grelet V, Dufour P, Nadri M, Lemort V, Reiche T, Tilman S. Model based control for waste heat recovery heat exchangers Rankine cycle system in heavy-duty trucks. *3RD Int. Semin. ORC Power Syst.*, Brussels, Belgium: 2015, p. 1–10.
- [54] Yousefzadeh M, Uzgoren E. Mass-conserving dynamic organic Rankine cycle model to investigate the link between mass distribution and system state. *Energy* 2015;93:1128–39. doi:10.1016/j.energy.2015.09.102.
- [55] Zhang J, Mifeng R, Jing X, Mingming L. Multi-objective Optimal Temperature Control for Organic Rankine Cycle Systems. *Proceeding 11th World Congr. Intell. Control Autom.*, Shenyang, China: 2014, p. 661–6.
- [56] Feru E, Willems F, de Jager B, Steinbuch M. Modeling and control of a parallel waste heat recovery system for Euro-VI heavy-duty diesel engines. *Energies* 2014;7:6571–92. doi:10.3390/en7106571.
- [57] Zhang J, Zhou Y, Wang R, Xu J, Fang F. Modeling and constrained multivariable predictive control for ORC (Organic Rankine Cycle) based waste heat energy conversion systems. *Energy* 2014;66:128–38. doi:10.1016/j.energy.2014.01.068.

- [58] Luong D, Tsao T. Model Predictive Control of Organic Rankine Cycle for Waste Heat Recovery in Heavy-Duty Diesel Powertrain. Proc. ASME 2014 Dyn. Syst. Control Conf. DSCC2014, San Antonio, TX, USA: 2014, p. 1–7.
- [59] Hou G, Bi S, Lin M, Zhang J, Xu J. Minimum variance control of organic Rankine cycle based waste heat recovery. *Energy Convers Manag* 2014;86:576–86. doi:10.1016/j.enconman.2014.06.004.
- [60] Peralez J, Tona P, Lepreux O, Sciarretta A, Voise L, Dufour P, et al. Improving the Control Performance of an Organic Rankine Cycle System for Waste Heat Recovery from a Heavy-Duty Diesel Engine using a Model-Based Approach. 52nd IEEE Conf. Decis. Control, vol. 7, Florence, Italy: 2013, p. 6830–6. doi:10.1109/CDC.2013.6760971.
- [61] Xie H, Yang C. Dynamic behavior of Rankine cycle system for waste heat recovery of heavy duty diesel engines under driving cycle. *Appl Energy* 2013;112:130–41. doi:10.1016/j.apenergy.2013.05.071.
- [62] Manente G, Toffolo A, Lazzaretto A, Paci M. An Organic Rankine Cycle off-design model for the search of the optimal control strategy. *Energy* 2013;58:97–106. doi:10.1016/j.energy.2012.12.035.
- [63] Peralez J, Tona P, Sciarretta A, Dufour P, Towards MN. Towards model-based control of a steam Rankine process for engine waste heat recovery. 2012 IEEE Veh. Power Propuls. Conf. (VPPC), Korea, Repub., 2012, p. 289–94. doi:10.1109/VPPC.2012.6422718.
- [64] Zhang J, Zhang W, Hou G, Fang F. Dynamic modeling and multivariable control of organic Rankine cycles in waste heat utilizing processes. *Comput Math with Appl* 2012;64:908–21. doi:10.1016/j.camwa.2012.01.054.
- [65] Chowdhury JI, Nguyen BK, Thornhill D. Dynamic model of supercritical organic rankine cycle waste heat recovery system for internal combustion engine. *Int J ...* 2012;13:293–300. doi:10.1007/s12239.
- [66] Espinosa N, Lemort V, Lombard B, Quoilin S. Transient Organic Rankine cycle Modelling for Waste Heat Recovery on a Truck. 24th Int. Conf. Effic. Cost, Optim. Simul. Environ. Impact Energy Syst., Serbia: 2011, p. 1–21.
- [67] Zhang Y, Deng S, Zhao L, Lin S, Bai M, Wang W, et al. Dynamic test and verification of model-guided ORC system. *Energy Convers Manag* 2019;186:349–67. doi:10.1016/j.enconman.2019.02.055.
- [68] Lie M, Habib B, Yu W, Wilson D, Young BR. Validating control of extreme disturbance of an organic Rankine cycle using VMGsim. *Comput Aided Chem Eng* 2018;44:745–50. doi:10.1016/B978-0-444-64241-7.50119-1.

- [69] Pili R, Spliethoff H, Wieland C. Dynamic Simulation of an Organic Rankine Cycle—Detailed Model of a Kettle Boiler. *Energies* 2017;10:548. doi:10.3390/en10040548.
- [70] Alobaid F, Mertens N, Starkloff R, Lanz T, Heinze C, Epple B. Progress in dynamic simulation of thermal power plants. *Prog Energy Combust Sci* 2017;59:79–162. doi:10.1016/j.peccs.2016.11.001.
- [71] Shin JY, Jeon YJ, Maeng DJ, Kim JS, Ro ST. Analysis of the dynamic characteristics of a combined-cycle power plant. *Energy* 2002;27:1085–98. doi:10.1016/S0360-5442(02)00087-7.
- [72] Bell IH, Quoilin S, Georges E, Braun JE, Groll E a., Horton WT, et al. A generalized moving-boundary algorithm to predict the heat transfer rate of counterflow heat exchangers for any phase configuration. *Appl Therm Eng* 2015;79:192–201. doi:10.1016/j.applthermaleng.2014.12.028.
- [73] Braun W, Casella F, Bachmann B. Solving large-scale Modelica models: new approaches and experimental results using OpenModelica. Proc 12th Int Model Conf Prague, Czech Republic, May 15-17, 2017 2017;132:557–63. doi:10.3384/ecp17132557.
- [74] Jensen JM. Dynamic Modeling of ThermoFluid Systems (PhD Thesis). 2003. doi:10.1017/CBO9781107415324.004.
- [75] Xu B, Rathod D, Kulkarni S, Yebi A, Filipi Z, Onori S, et al. Transient dynamic modeling and validation of an organic Rankine cycle waste heat recovery system for heavy duty diesel engine applications. *Appl Energy* 2017;205:260–79. doi:10.1016/j.apenergy.2017.07.038.
- [76] Desideri A, Dechesne B, Wronski J, van den Broek M, Gusev S, Lemort V, et al. Comparison of Moving Boundary and Finite-Volume Heat Exchanger Models in the Modelica Language. *Energies* 2016;9:339. doi:10.3390/en9050339.
- [77] Quoilin S, Bell I, Desideri A, Dewallef P, Lemort V. Methods to increase the robustness of finite-volume flow models in thermodynamic systems. *Energies* 2014;7:1621–40. doi:10.3390/en7031621.
- [78] Quoilin S. Sustainable energy conversion through the use of organic rankine cycles for waste heat recovery and solar applications. University of Liège, 2011.
- [79] Adriano Desideri. Dynamic Modeling of Organic Rankine Cycle Power Systems. Université de Liège, 2016.
- [80] Hefni B El, Bouskela D, Gentilini G. Dynamic modelling of a Condenser/Water Heater with the {ThermoSysPro} Library. Proc. 9th Int. {MODELICA} Conf. Sept. 3-5, 2012, Munich, Ger., Linköping University Electronic Press; 2012. doi:10.3384/ecp12076745.
- [81] Li P, Li Y, Seem JE. Dynamic modeling and consistent initialization of system of differential-

- algebraic equations for centrifugal chillers. Fourth Natl. Conf. IBPSA-USA, New York City, USA: 2010, p. 386–93.
- [82] Lemort V, Quoilin S, Cuevas C, Lebrun J. Testing and modeling a scroll expander integrated into an organic rankine cycle. *Appl Therm Eng* 2009;29:3094–102. doi:10.1016/j.applthermaleng.2009.04.013.
- [83] Casella F. Dynamic modeling and control of Organic Rankine Cycle plants. *Org. Rank. Cycle Power Syst.*, Elsevier Ltd; 2017, p. 153–71. doi:10.1016/B978-0-08-100510-1.00006-5.
- [84] Quoilin S, Lemort V, Lebrun J. Experimental study and modeling of an Organic Rankine Cycle using scroll expander. *Appl Energy* 2010;87:1260–8. doi:10.1016/j.apenergy.2009.06.026.
- [85] Stodola A. *Dampf- und Gasturbinen: Mit einem Anhang über die Aussichten der Wärmekraftmaschinen*; Springer: Berlin, Germany. 1922:1922.
- [86] Vetter G. *Rotierende Verdrängerpumpen für die Prozesstechnik Gebundene*, Vulkan; 2006, p. 64.
- [87] Zhu Y, Verhaegen M. Subspace Model Identification of MIMO Processes. *Multivariable Syst. Identif. Process Control*, Pergamon; 2001, p. 199–216. doi:10.1016/B978-008043985-3/50010-7.
- [88] Grelet V, Dufour P, Nadri M, Reiche T, Lemort V. Modeling and control of Rankine based waste heat recovery systems for heavy duty trucks. *IFAC-PapersOnLine* 2015;48:568–73. doi:10.1016/j.ifacol.2015.09.028.
- [89] Casella F, Colonna P. Dynamic modeling of IGCC power plants. *Appl Therm Eng* 2012;35:91–111. doi:https://doi.org/10.1016/j.applthermaleng.2011.10.011.
- [90] Tică A, Guéguen H, Dumur D, Faille D, Davelaar F. Design of a combined cycle power plant model for optimization. *Appl Energy* 2012;98:256–65. doi:https://doi.org/10.1016/j.apenergy.2012.03.032.
- [91] Sindareh-Esfahani P, Habibi-Siyahposh E, Saffar-Avval M, Ghaffari A, Bakhtiari-Nejad F. Cold start-up condition model for heat recovery steam generators. *Appl Therm Eng* 2014;65:502–12. doi:https://doi.org/10.1016/j.applthermaleng.2014.01.016.
- [92] Camporeale SM, Fortunato B, Mastrovito M. A Modular Code for Real Time Dynamic Simulation of Gas Turbines in Simulink. *J Eng Gas Turbines Power* 2002;128:506–17. doi:10.1115/1.2132383.
- [93] Haryanto A, Hong K-S. Modeling and simulation of an oxy-fuel combustion boiler system with flue gas recirculation. *Comput Chem Eng* 2011;35:25–40. doi:https://doi.org/10.1016/j.compchemeng.2010.05.001.

- [94] Bhambare KS, Mitra SK, Gaitonde UN. Modeling of a Coal-Fired Natural Circulation Boiler. *J Energy Resour Technol* 2006;129:159–67. doi:10.1115/1.2719209.
- [95] Lu S. Dynamic modelling and simulation of power plant systems. *Proc Inst Mech Eng Part A J Power Energy* 1999;213:7–22. doi:10.1243/0957650991537392.
- [96] Garcia HE, Chen J, Kim JS, Vilim RB, Binder WR, Bragg Sitton SM, et al. Dynamic performance analysis of two regional Nuclear Hybrid Energy Systems. *Energy* 2016;107:234–58. doi:https://doi.org/10.1016/j.energy.2016.03.128.
- [97] Zio E, Maio F Di. Processing dynamic scenarios from a reliability analysis of a nuclear power plant digital instrumentation and control system. *Ann Nucl Energy* 2009;36:1386–99. doi:https://doi.org/10.1016/j.anucene.2009.06.012.
- [98] Li H, Huang X, Zhang L. A simplified mathematical dynamic model of the HTR-10 high temperature gas-cooled reactor with control system design purposes. *Ann Nucl Energy* 2008;35:1642–51. doi:https://doi.org/10.1016/j.anucene.2008.02.012.
- [99] Wan J, Song H, Yan S, Sun J, Zhao F. Development of a simulation platform for dynamic simulation and control studies of AP1000 nuclear steam supply system. *Ann Nucl Energy* 2015;85:704–16. doi:https://doi.org/10.1016/j.anucene.2015.06.026.
- [100] Liu SJ, Faille D, Fouquet M, El-Hefni B, Wang Y, Zhang JB, et al. Dynamic Simulation of a 1MWe CSP Tower Plant with Two-level Thermal Storage Implemented with Control System. *Energy Procedia* 2015;69:1335–43. doi:https://doi.org/10.1016/j.egypro.2015.03.139.
- [101] Bonilla J, Yebra LJ, Dormido S, Zarza E. Parabolic-trough solar thermal power plant simulation scheme, multi-objective genetic algorithm calibration and validation. *Sol Energy* 2012;86:531–40. doi:https://doi.org/10.1016/j.solener.2011.10.025.
- [102] Singh R, Rowlands AS, Miller SA. Effects of relative volume-ratios on dynamic performance of a direct-heated supercritical carbon-dioxide closed Brayton cycle in a solar-thermal power plant. *Energy* 2013;55:1025–32. doi:https://doi.org/10.1016/j.energy.2013.03.049.
- [103] Zhang J, Li K, Xu J. Recent developments of control strategies for organic Rankine cycle (ORC) systems. *Trans Inst Meas Control* 2018. doi:10.1177/0142331217753061.
- [104] Quoilin S, Orosz M, Lemort V. Modeling and experimental investigation of an Organic Rankine Cycle using scroll expander for small scale solar applications. *EUROSUN 1st Int Conf Sol Heating, Cool Build* 2008:1–8.
- [105] Corriou J-P. *Process Control : Theory and Applications*. 2nd ed. Springer; 2018.
- [106] Ziegler JG, Nichols NB. Optimum settings for automatic controllers. *Trans ASME* 1942;64:759–68. doi:10.1115/1.2899060.

- [107] Powell WB. *Approximate Dynamic Programming: Solving the Curses of Dimensionality: Second Edition*. Wiley-Blackwell; 2011. doi:10.1002/9781118029176.
- [108] Fernandez-Camacho E, Bordons-Alba C. *Model predictive control in the process industry*. Springer-Verlag London; 1996. doi:10.1007/978-1-4471-3008-6.
- [109] Luong D, Tsao T. Control of a base load and load-following regulating Organic rankine cycle for waste heat recovery in heavy-duty diesel powertrain. *ASME 2015 Dyn. Syst. Control Conf.*, 2017, p. 1–9.
- [110] MATLAB (2017a). *Simulink: MathWorks, Inc., Natick, Massachusetts, United States*. 2017.
- [111] Usman M, Imran M, Lee DH, Park B-S. Experimental investigation of off-grid organic Rankine cycle control system adapting sliding pressure strategy under proportional integral with feed-forward and compensator. *Appl Therm Eng* 2017;110:1153–63. doi:10.1016/j.applthermaleng.2016.09.021.
- [112] Pili R, Romagnoli A, Jiménez-Arreola M, Spliethoff H, Wieland C. Simulation of Organic Rankine Cycle – Quasi-steady state vs dynamic approach for optimal economic performance. *Energy* 2019;167:619–40. doi:10.1016/J.ENERGY.2018.10.166.
- [113] Pili R, Spliethoff H, Wieland C. Effect of cold source conditions on the design and control of organic rankine cycles for waste heat recovery from industrial processes. *ECOS 2019 - Proc 32nd Int Conf Effic Cost, Optim Simul Environ Impact Energy Syst* 2019:3039–51.
- [114] Lin S, Zhao L, Deng S, Ni J, Zhang Y, Ma M. Dynamic performance investigation for two types of ORC system driven by waste heat of automotive internal combustion engine. *Energy* 2019;169:958–71. doi:10.1016/J.ENERGY.2018.12.092.
- [115] Marchionni M, Bianchi G, Karvountzis-Kontakiotis A, Pesyridis A, Tassou SA. An appraisal of proportional integral control strategies for small scale waste heat to power conversion units based on Organic Rankine Cycles. *Energy* 2018;163:1062–76. doi:10.1016/j.energy.2018.08.156.
- [116] Imran M, Haglind F. Dynamic modelling and development of a reliable control strategy of organic Rankine cycle power systems for waste heat recovery on heavy-duty vehicles. *Proc. 32nd Int. Conf. Effic. Cost, Optim. Simul. Environ. Impact Energy Syst. Wroclaw, Poland, 23-28 June, Wroclaw, Poland: 2019*.
- [117] Yang C, Wang W, Xie H. An efficiency model and optimal control of the vehicular diesel exhaust heat recovery system using an organic Rankine cycle. *Energy* 2019;171:547–55. doi:10.1016/j.energy.2018.12.219.
- [118] Peralez J, Tona P, Sciarretta A, Dufour P, Nadri M. Optimal control of a vehicular organic rankine

- cycle via dynamic programming with adaptive discretization grid. Proc. 19th World Congr. Int. Fed. Autom. Control, vol. 19, Cape Town, South Africa: IFAC; 2014, p. 5671–8. doi:10.3182/20140824-6-ZA-1003.02185.
- [119] Peralez J, Tona P, Nadri M, Dufour P, Sciarretta A. Optimal control for an organic rankine cycle on board a diesel-electric railcar. *J Process Control* 2015;33:1–13. doi:10.1016/j.jprocont.2015.03.009.
- [120] Zhang J, Ren M, Yue H. Constrained entropy-based temperature control of waste heat systems. Proc. World Congr. Intell. Control Autom., 2016, p. 1992–8. doi:10.1109/WCICA.2016.7578809.
- [121] Zhang J, Tian X, Zhu Z, Ren M. Data-Driven Superheating Control of Organic Rankine Cycle Processes. Hindawi Complex 2018;2018.
- [122] Zhang J, Lin M, Shi F, Meng J, Xu J. Set point optimization of controlled Organic Rankine Cycle systems. *Chinese Sci Bull* 2014;59:4397–404. doi:10.1007/s11434-014-0590-1.
- [123] Hoang N-D, Tien Bui D. Slope Stability Evaluation Using Radial Basis Function Neural Network, Least Squares Support Vector Machines, and Extreme Learning Machine. *Handb. Neural Comput.*, Academic Press; 2017, p. 333–44. doi:10.1016/B978-0-12-811318-9.00018-1.
- [124] Xialai W, Lei X, Junghui C, Hongye S, Xiaochen L. An Optimal Control Design of Organic Rankine Cycle under Disturbances. 37th Chinese Control Conf., Wuhan, China: Technical Committee on Control Theory, Chinese Association of Automation; 2018, p. 3475–80.
- [125] Ren M, Cheng T, Cheng L, Yan G, Zhang J. A single neuron controller for non-Gaussian systems with unmodeled dynamics. *UKACC Int Conf Control UKACC Control 2016* 2016. doi:10.1109/CONTROL.2016.7737554.
- [126] Luong D, Tsao T. Linear Quadratic Integral Control of an Organic Rankine Cycle for Waste Heat Recovery in Heavy-Duty Diesel Powertrain. Proc. ASME 2014 Dyn. Syst. Control Conf. DSCC2014, San Antonio, TX, USA: 2014, p. 1–7. doi:10.1109/ACC.2014.6858907.
- [127] Hernandez A, Ruiz F, Desideri A, Ionescu C, Quoilin S, Lemort V, et al. Nonlinear identification and control of Organic Rankine Cycle systems using sparse polynomial models. *2016 IEEE Conf Control Appl CCA 2016* 2016:1012–7. doi:10.1109/CCA.2016.7587946.
- [128] Hernandez A, Desideri A, Ionescu C, Quoilin S, Lemort V, De Keyser R. Increasing the efficiency of Organic Rankine Cycle Technology by means of Multivariable Predictive Control. *IFAC Proc Vol* 2014;47:2195–200. doi:10.3182/20140824-6-ZA-1003.01796.
- [129] Hernandez A, Desideri A, Ionescu C, Quoilin S, Lemort V, Keyser R De. Experimental study of Predictive Control strategies for optimal operation of Organic Rankine Cycle systems. *2015 Eur. Control Conf.*, Linz, Austria: 2015, p. 2259–64.

- [130] Zhang J, Zhang T, Lin M, Hou G, Li K. Multiple Model Predictive Control for Organic Rankine Cycle (ORC) based Waste Heat Energy Conversion Systems. 2016 UKACC 11th Int. Conf. Control, Belfast: 2016, p. 1–7.
- [131] Pierobon L, Chan R, Li X, Iyengar K, Haglind F, Ydstie E. Model Predictive Control of Offshore Power Stations With Waste Heat Recovery. *J Eng Gas Turbines Power* 2016;138:71801.
- [132] Rahmani MA, Alamir M, Gualino D, Rieu V. Nonlinear Dynamic Model Identification and MPC control of an Organic Rankine Cycle (ORC) based Solar Thermal Power Plant. 2015 Eur. Control Conf., Linz, Austria: 2015, p. 2544–51.
- [133] Grelet V, Dufour P, Nadri M, Lemort V, Reiche T. Explicit multi-model predictive control of a waste heat Rankine based system for heavy duty trucks. *Proc IEEE Conf Decis Control* 2015;54rd IEEE:179–84. doi:10.1109/CDC.2015.7402105.
- [134] Petr P, Schröder C, Köhler J, Gräber M. Optimal control of waste heat recovery systems applying nonlinear model predictive control (NMPC). 3RD Int. Semin. ORC Power Syst. Oct. 12-14, 2015, Brussels, Belgium, Brussels, Belgium: 2015, p. 1–10.
- [135] Hilding Elmqvist. Modelica — A unified object-oriented language for physical systems modeling. *Simul Pract Theory* 1997. doi:10.1016/s0928-4869(97)84257-7.
- [136] Hernandez A, Desideri A, Gusev S, Ionescu CM, Den Broek M Van, Quoilin S, et al. Design and experimental validation of an adaptive control law to maximize the power generation of a small-scale waste heat recovery system. *Appl Energy* 2017;203:549–59. doi:10.1016/j.apenergy.2017.06.069.
- [137] Wu X, Chen J, Xie L. Fast economic nonlinear model predictive control strategy of Organic Rankine Cycle for waste heat recovery: Simulation-based studies. *Energy* 2019;180:520–34. doi:10.1016/j.ENERGY.2019.05.023.
- [138] Koppauer H, Kemmetmüller W, Kugi A. Model predictive control of an automotive waste heat recovery system. *Control Eng Pract* 2018;81:28–42. doi:10.1016/j.CONENGPRAC.2018.09.005.
- [139] Rathod D, Xu B, Filipi Z, Hoffman M. An experimentally validated, energy focused, optimal control strategy for an Organic Rankine Cycle waste heat recovery system. *Appl Energy* 2019;256:113991. doi:10.1016/J.APENERGY.2019.113991.
- [140] Zhang J, Zhou Y, Li Y, Hou G, Fang F. Generalized predictive control applied in waste heat recovery power plants. *Appl Energy* 2013;102:320–6. doi:10.1016/j.apenergy.2012.07.038.
- [141] Zhang J, Feng J, Zhou Y, Fang F, Yue H. Linear active disturbance rejection control of waste heat recovery systems with organic Rankine cycles. *Energies* 2012;5:5111–25. doi:10.3390/en5125111.

- [142] Yebi A, Xu B, Liu X, Shutty J, Anshel P, Filipi Z, et al. Estimation and predictive control of a parallel evaporator diesel engine waste heat recovery system. *IEEE Trans Control Syst Technol* 2019;27:282–95. doi:10.1109/TCST.2017.2759104.
- [143] Hernandez A, Desideri A, Ionescu C, De Keyser R, Lemort V, Quoilin S. Real-Time Optimization of Organic Rankine Cycle Systems by Extremum-Seeking Control. *Energies* 2016;9:334. doi:10.3390/en9050334.
- [144] Zhang J, Song G, Yannan C, Guolian H. Multivariable Robust Control for Organic Rankine Cycle Based Waste Heat Recovery Systems. *IEEE 8th Conf. Ind. Electron. Appl.*, 2013, p. 85–9.
- [145] Wang R, Wang C, Zhao X, Zhang W. Neuro-PID control of heat exchanger in an Organic Rankine Cycle system for waste heat recovery. *2011 Int Conf Adv Mechatron Syst* 2011:191–5.
- [146] Torregrosa A, Galindo J, Dolz V, Royo-Pascual L, Haller R, Melis J. Dynamic tests and adaptive control of a bottoming organic Rankine cycle of IC engine using swash-plate expander. *Energy Convers Manag* 2016;126:168–76. doi:10.1016/j.enconman.2016.07.078.
- [147] Padula F, Sandrini R, Cominardi G, Cominardi FPRSG. Adaptive PI Control of an Organic Rankine Cycle Power Plant. vol. 45. *IFAC; 2012*. doi:10.3182/20120328-3-IT-3014.00078.
- [148] Imran M, Haglind F, Lemort V, Meroni A. Optimization of organic rankine cycle power systems for waste heat recovery on heavy-duty vehicles considering the performance, cost, mass and volume of the system. *Energy* 2019;180:229–41. doi:10.1016/J.ENERGY.2019.05.091.
- [149] Zhang J, Lin M, Fang F, Xu J, Li K. Gain scheduling control of waste heat energy conversion systems based on an LPV (linear parameter varying) model. *Energy* 2016;107:773–83. doi:10.1016/j.energy.2016.04.064.
- [150] Grelet V, Dufour P, Nadri M, Lemort V, Reiche T. Explicit multi-model predictive control of a waste heat Rankine based system for heavy duty trucks. *Conf Decis Control (CDC)2* 2015:179–84.